# ASelaginella moellendorffiiOrtholog of KARRIKIN INSENSITIVE2 Functions in Arabidopsis Development but Cannot Mediate Responses to Karrikins or Strigolactones

Mark T. Waters, Adrian Scaffidi, Solène Y. Moulin, Yueming K. Sun, Gavin R. Flematti, Steven M. Smith

The Plant Cell, Vol. 27: 1925–1944, July 2015, www.plantcell.org 

# A *Selaginella moellendorffii* Ortholog of KARRIKIN INSENSITIVE2 Functions in Arabidopsis Development but Cannot Mediate Responses to Karrikins or Strigolactones[OPEN]

**Mark T. Waters,[a,1] Adrian Scaffidi,[b] Solène L.Y. Moulin,[a] Yueming K. Sun,[a] Gavin R. Flematti,[b] and Steven M. Smith[a,b,c]**

[a] Australian Research Council Centre of Excellence for Plant Energy Biology, The University of Western Australia, Perth, Western Australia 6009, Australia

[b] School of Chemistry and Biochemistry, The University of Western Australia, Perth, Western Australia 6009, Australia

[c] School of Biological Sciences, University of Tasmania, Hobart, Tasmania 7001, Australia

ORCID IDs: 0000-0001-5657-9005 (M.T.W.); 0000-0002-7347-1247 (S.L.Y.M.); 0000-0002-8605-5955 (Y.K.S.); 0000-0001-5661-9994 (S.M.S.)

**In *Arabidopsis thaliana*, the α/β-fold hydrolase KARRIKIN INSENSITIVE2 (KAI2) is essential for normal seed germination, seedling development, and leaf morphogenesis, as well as for responses to karrikins. KAI2 is a paralog of DWARF14 (D14), the proposed strigolactone receptor, but the evolutionary timing of functional divergence between the KAI2 and D14 clades has not been established. By swapping gene promoters, we show that Arabidopsis KAI2 and D14 proteins are functionally distinct. We show that the catalytic serine of KAI2 is essential for function in plants and for biochemical activity in vitro. We identified two KAI2 homologs from *Selaginella moellendorffii* and two from *Marchantia polymorpha*. One from each species could hydrolyze the strigolactone analog GR24 in vitro, but when tested for their ability to complement Arabidopsis *d14* and *kai2* mutants, neither of these homologs was effective. However, the second KAI2 homolog from *S. moellendorffii* was able to complement the seedling and leaf development phenotypes of Arabidopsis *kai2*. This homolog could not transduce signals from exogenous karrikins, strigolactone analogs, or carlactone, but its activity did depend on the conserved catalytic serine. We conclude that KAI2, and most likely the endogenous signal to which it responds, has been conserved since the divergence of lycophytes and angiosperm lineages, despite their major developmental and morphogenic differences.**

## INTRODUCTION

Historically, observations of the effects of exogenous compounds on plant growth have often initiated the discovery of hormone signaling pathways. A decade ago, karrikins were revealed as a group of compounds that are generated from the burning of plant matter and promote postfire seed germination (Flematti et al., 2004). Six members of the karrikin family have been identified from smoke, among which $KAR_1$ and $KAR_2$ are generally the most active (Flematti et al., 2009; Nelson et al., 2012). Chemically classified as butenolides, karrikins share structural similarity with strigolactones (SLs), a group of carotenoid-derived plant hormones that were first isolated as seed germination stimulants of root-parasitic weeds in the Orobanchaceae (Cook et al., 1966). Subsequently, SLs have been demonstrated to regulate axillary shoot branching and numerous other aspects of plant development (Waldie et al., 2014). In *Arabidopsis thaliana*, both karrikins and the synthetic SL GR24 can accelerate germination of primary dormant seed, and both enhance the light responses of seedlings, such as the inhibition of hypocotyl elongation (Nelson et al., 2009, 2010). However, karrikins cannot stimulate the germination of parasitic weed seeds and have no effect on shoot architecture (Nelson et al., 2011), indicating that karrikins and SLs are superficially similar but functionally distinct compounds.

To date, genetic studies in Arabidopsis have led to the discovery of three proteins required for plant responses to karrikins. The first, F-box protein MORE AXILLARY BRANCHES2 (MAX2), was identified in a screen for karrikins-insensitive (*kai*) mutants. As MAX2 was already implicated in mediating responses to SL, this finding provided the first genetic evidence that the response pathways to karrikins and SLs have components in common (Nelson et al., 2011). Further parallels between karrikin and SL signaling were established following the identification of the second key protein KAI2, a paralog of rice (*Oryza sativa*) DWARF14 (D14). D14 and its orthologs in petunia (*Petunia hybrida*; DECREASED APICAL DOMINANCE2 [DAD2]) and Arabidopsis (D14) are α/β-fold hydrolases essential for the SL response, and D14 is now widely considered the SL receptor (Arite et al., 2009; Hamiaux et al., 2012; Waters et al., 2012a; Bennett and Leyser, 2014; Chevalier et al., 2014). In Arabidopsis, KAI2 is necessary for all karrikin responses but is not required for SL responses (Waters et al., 2012a; Scaffidi et al., 2014), explaining one way by which plants distinguish between these two classes of bioactive butenolides. Direct interaction between KAI2 and karrikins has been inferred from isothermal calorimetry (Kagiyama et al., 2013) and crystallography (Guo et al., 2013),

[1] Address correspondence to mark.waters@uwa.edu.au.
The author responsible for distribution of materials integral to the findings presented in this article in accordance with the policy described in the Instructions for Authors (www.plantcell.org) is: Mark T. Waters (mark.waters@uwa.edu.au).
[OPEN]Articles can be viewed online without a subscription.
www.plantcell.org/cgi/doi/10.1105/tpc.15.00146

implicating a receptor role for KAI2. Third, SUPPRESSOR OF MAX2 1 (SMAX1), a protein with weak homology to Clp ATPases and HEAT SHOCK PROTEIN 101, was identified as a component of karrikin signaling that likely acts downstream of MAX2 (Stanga et al., 2013). Most recently, D53, a homolog of SMAX1 in rice, has been described as a key component of SL signaling that interacts with D14 and D3, the rice ortholog of MAX2 (Jiang et al., 2013; Zhou et al., 2013). MAX2/D3 is an F-box protein that associates with Skp1 and Cullin1 homologs to form an E3 ubiquitin-protein ligase complex termed $SCF^{MAX2/D3}$ (Ishikawa et al., 2005; Stirnberg et al., 2007). SCF complexes ubiquitinate specific proteins and target them for proteasomal degradation (Deshaies and Joazeiro, 2009). D53 is degraded by SLs through a D14- and D3-dependent mechanism, most probably via this ubiquitin-proteasome system (Jiang et al., 2013; Zhou et al., 2013). SMAX1 and D53 define a small family (SMAX-like or SMXL) of otherwise uncharacterized proteins, which together with two different receptor proteins (KAI2 and D14) could operate in a combinatorial fashion to modulate different aspects of development (Smith and Li, 2014). Thus, responses to karrikins and SLs come about through broadly analogous mechanisms: An $\alpha/\beta$-fold hydrolase perceives a ligand, which activates $SCF^{MAX2/D3}$ and in turn promotes the proteasomal degradation of repressor proteins in the SMXL family (Jiang et al., 2013; Stanga et al., 2013; Waters et al., 2013; Zhou et al., 2013).

Recessive, loss-of-function karrikin-insensitive mutants, namely, *kai2* and *max2*, share a number of informative phenotypes. Freshly harvested seeds of both have germination rates lower than the wild type. Seedlings of both genotypes exhibit impaired photomorphogenesis, with elongated hypocotyls and small, epinastic cotyledons. Third, *kai2* and *max2* both share aberrant expression of a number of transcriptional markers. Notably, the direction and nature of these distinctive phenotypes are opposite to the effects of karrikin application. Together, these phenotypes imply that the KAI2-MAX2 signaling system plays an important developmental role even in the absence of exogenous karrikins. Given that D14 is the likely SL receptor, these observations imply that the *kai2* and *max2* phenotypes result from the inability to perceive an unknown signaling compound that is the substrate or ligand for KAI2. The presumed KAI2 ligand is currently unknown; however, while it is likely to be a butenolide, it is probably not derived from the canonical SL biosynthetic pathway for two reasons. First, carlactone, a precursor of all known SLs, cannot influence seedling development through KAI2 (Scaffidi et al., 2013). Second, KAI2 cannot perceive the natural SLs 5-deoxystrigol (5DS) and 4-deoxyorobanchol, while D14 can (Scaffidi et al., 2014). Curiously, both proteins mediate responses to GR24, which is typically synthesized and used as a racemic mixture of two enantiomers (i.e., *rac*-GR24). One of these enantiomers exhibits the same stereochemistry as 5DS ($GR24^{5DS}$), while the other is its mirror image with no known natural equivalent ($GR24^{ent\text{-}5DS}$). We now understand that *rac*-GR24 activity derives from the combined responses to each enantiomer, $GR24^{5DS}$ and $GR24^{ent\text{-}5DS}$, mediated primarily by D14 and KAI2, respectively (Scaffidi et al., 2014). Thus, KAI2 does not perceive SLs with natural stereochemistry and must have different ligand requirements to D14.

As $\alpha/\beta$-fold hydrolases, both KAI2 and D14 possess a conserved catalytic triad of serine, histidine, and aspartic acid residues within a hydrophobic active site. In D14, this triad is essential for function because a mutant D14 lacking the catalytic serine is unable to complement the *d14* shoot branching phenotype and cannot hydrolyze GR24 in vitro (Hamiaux et al., 2012). In addition, mutant D14 does not exhibit GR24-dependent association with D53 (Jiang et al., 2013). It is thought that hydrolysis of SL induces a conformational change in D14, permitting the formation of a complex between D14, MAX2/D3, and SMXL proteins. The degree to which these signaling events involving D14 are also true for KAI2 is currently unclear. First, unlike SLs, the molecular nature of karrikins is such that they are not expected to yield a new hydrolysis product (Scaffidi et al., 2012; Waters et al., 2014), and structural studies indicate that karrikins bind within the hydrophobic cavity of KAI2, but insufficiently close to the catalytic serine to undergo nucleophilic attack (Guo et al., 2013). This binding position was reported to change the overall shape of the KAI2 protein, thus implying that karrikins might signal independently of any hydrolytic activity of KAI2. Second, it has not been conclusively demonstrated that the different in planta activities of KAI2 and D14 are intrinsic to the proteins themselves or are due to spatiotemporal differences in expression or regulation.

The KAI2-D14 family of $\alpha/\beta$-fold hydrolases is represented in all major land plant taxa, as well as in charophyte algae, but true D14 orthologs are restricted to seed plants (Delaux et al., 2012; Waters et al., 2012a). This lack of D14 orthologs in non-seed plants has prompted speculation that D14 arose from a gene duplication event prior to the emergence of seed plants, permitting functional specialization between KAI2 and D14 (Waters et al., 2013). The lycophyte *Selaginella moellendorffii* (date of divergence ~400 to 430 million years ago) and the liverwort *Marchantia polymorpha* (~450 to 470 million years ago) are emerging model species for studying the development of basal land plants, and genomic sequence data for these species are either complete or underway (Banks et al., 2011; Bowman, 2013). Curiously, the production of SLs has been reported in *M. polymorpha* (Delaux et al., 2012), *Physcomitrella patens* (Proust et al., 2011), and in the charophyte alga *Nitella mirabilis* (Delaux et al., 2012), suggesting that SL synthesis predates the appearance of D14 in seed plants (which emerged >360 million years ago) by at least 100 million years. It has been suggested that the evolution of D14 has coincided with increased developmental complexity and the adoption of SLs as a hormonal signal to regulate diverse aspects of plant growth (Waters et al., 2013; Waldie et al., 2014). Assuming SLs have a hormonal function in basal land plants, KAI2 homologs could serve as potential SL receptor proteins in these species. Alternatively, these KAI2 proteins may serve an ancestral function independent of SLs, instead operating with another ligand that is still present in modern-day angiosperms. One prediction of this latter hypothesis is that KAI2 function would be conserved between species over a large evolutionary timescale but that D14 function would not. More broadly, comparing the relative conservation of related signaling systems will add to our understanding of when and how developmental innovations occurred during land plant evolution.

In this study, we examine the functional characteristics of KAI2 in Arabidopsis and use biochemical and transgenic approaches to investigate the degree to which KAI2 function is evolutionarily conserved among diverse land plant taxa.

## RESULTS

### Arabidopsis D14 Cannot Substitute for KAI2 in the Control of Seed Germination and Seedling Development

The *kai2* mutant phenotype demonstrates that KAI2 mediates the stimulation of seed germination by *rac*-GR24. Moreover, *D14* transcripts are only very weakly expressed in seeds, being up to 100-fold less abundant than *KAI2* transcripts (Waters et al., 2012a). However, D14 does mediate responses to *rac*-GR24 in seedlings and in the control of shoot branching, demonstrating that *rac*-GR24, or more specifically the $GR24^{5DS}$ stereoisomer, is a suitable ligand for D14 (Waters et al., 2012a; Scaffidi et al., 2014). Therefore, it is possible that the inability of D14 to mediate seed germination responses to *rac*-GR24 is a consequence of the low level of *D14* transcripts. To establish whether the differential functions of KAI2 and D14 result from spatiotemporal differences in expression, we designed a strategy to substitute KAI2 and D14 for each other, by reciprocal exchange of the gene promoter and coding regions. Thus, we generated *KAI2pro:D14* and *D14pro:KAI2* transgenes, together with *KAI2pro:KAI2* and *D14pro:D14* controls (Figure 1A).

Three independent, homozygous transgenic lines for *KAI2pro:KAI2* and three for *KAI2pro:D14* were established in the *kai2-2* mutant background. In seeds, expression of each transgene resulted in *KAI2* and *D14* transcripts at levels similar to native *KAI2* transcripts in wild-type Landsberg *erecta* (L*er*) seed (Figure 1B). Most notably, the *KAI2pro:D14* transgene led to the accumulation of *D14* transcripts at 36- to 50-fold higher levels than in wild-type seeds, suggesting that the activity of the transgenic *KAI2* promoter fragment is sufficient to mimic that of the native promoter in seeds.

Next, we assessed the ability of the two transgenes to reduce primary dormancy of *kai2-2* seed and to restore responsiveness of the seed to $KAR_2$ and *rac*-GR24. The *KAI2pro:KAI2* transgene fully complemented the *kai2-2* phenotype, restoring germination levels above those seen in L*er* on water-agar alone and restoring sensitivity to germination stimulants (Figure 1C). This apparent reduction in primary dormancy below that seen in L*er* might result from spatio-temporal differences in expression between the endogenous *KAI2* gene and the *KAI2pro:KAI2* transgene, which lacks the native genetic context of *KAI2*. Consistent with this possibility, seed of three homozygous lines overexpressing *KAI2* from the *35S* promoter exhibited a similar reduction in primary dormancy on water-agar (Supplemental Figure 1). In addition, these seed germinated more rapidly in response to $KAR_2$ and *rac*-GR24 relative to L*er* in line with KAI2 expression level. Thus, differences in *KAI2* expression are sufficient to modulate seed germination behavior. However, expression of *KAI2pro:D14* was unable to restore germination of *kai2-2* to wild-type levels and, most notably, did not confer any response to *rac*-GR24 despite the increased abundance of *D14* transcripts (Figure 1C). This result implies that relatively low expression of *D14* is insufficient to explain why only KAI2, and not D14, has a role in promoting germination in wild-type Arabidopsis seed. Furthermore, it implies that D14 is unable to replace KAI2 in the MAX2-dependent signaling cascade that regulates seed germination.

In Arabidopsis seedlings, loss of KAI2 function leads to impaired hypocotyl and cotyledon morphogenesis, but loss of D14 does not result in a visible phenotype at this stage of development. To investigate whether this apparent lack of role for D14 in seedling development results from differential spatiotemporal regulation of KAI2 and D14, we examined the developmental phenotypes and karrikin responses of *KAI2pro:D14* transgenic seedlings. As expected, the *KAI2pro:KAI2* transgene complemented the cotyledon and hypocotyl defects of *kai2-2* seedlings (Figure 1D). However, *KAI2pro:D14* seedlings remained morphologically indistinguishable from *kai2-2*. In addition, hypocotyl elongation in seedlings expressing the *KAI2pro:D14* transgene exhibited no responses to karrikins, unlike controls with the *KAI2pro:KAI2* transgene, which were fully responsive (Figure 1E). Finally, the levels of four KAI2-dependent transcripts in *KAI2pro:D14* seedlings were essentially unchanged relative to *kai2-2* seedlings, while those in *KAI2pro:KAI2* seedlings were all restored to a large extent (Figure 1F). These findings demonstrate that, like in seed, D14 cannot functionally replace KAI2, either in terms of the native signaling function of KAI2 or with respect to karrikin signaling.

### KAI2 Cannot Replace D14 in the Control of Primary Shoot Branching

Arabidopsis *d14* mutants exhibit increased numbers of primary shoot branches due to a lack of inhibition of rosette axillary meristems (Waters et al., 2012a; Chevalier et al., 2014). These mutants also show reduced stature and altered leaf morphology, in which both the petiole and lamina are shorter than equivalent wild-type leaves, thus giving the adult rosette a more compact appearance. As KAI2 shows some limited activity toward natural strigolactones in Arabidopsis hypocotyl elongation assays (Scaffidi et al., 2014), we asked whether KAI2, when ectopically expressed in the native domain of D14, could function in place of D14 in the regulation of secondary shoot growth and leaf morphogenesis. As expected, *D14pro:D14* transgenic plants bore leaves with wild-type shape, fully complementing the *d14-1* phenotype (Figure 2A). By contrast, the leaf and rosette appearance of *D14pro:KAI2* plants were indistinguishable from *d14-1* controls (Figure 2A). Likewise, the rosette branching phenotype of *D14pro:KAI2* plants was not significantly different from that of *d14-1*, but this aspect of growth was fully restored in *D14pro:D14* plants (Figures 2B and 2C). Thus, the functional differences between D14 and KAI2 are intrinsic to the proteins themselves and not due to differences in timing or location of gene expression.

### Ser-95 and Gly-133 Are Essential for Arabidopsis KAI2 Function in Planta

The catalytic triad of D14 is essential for responses to endogenous SLs and *rac*-GR24 (Hamiaux et al., 2012; Jiang et al.,

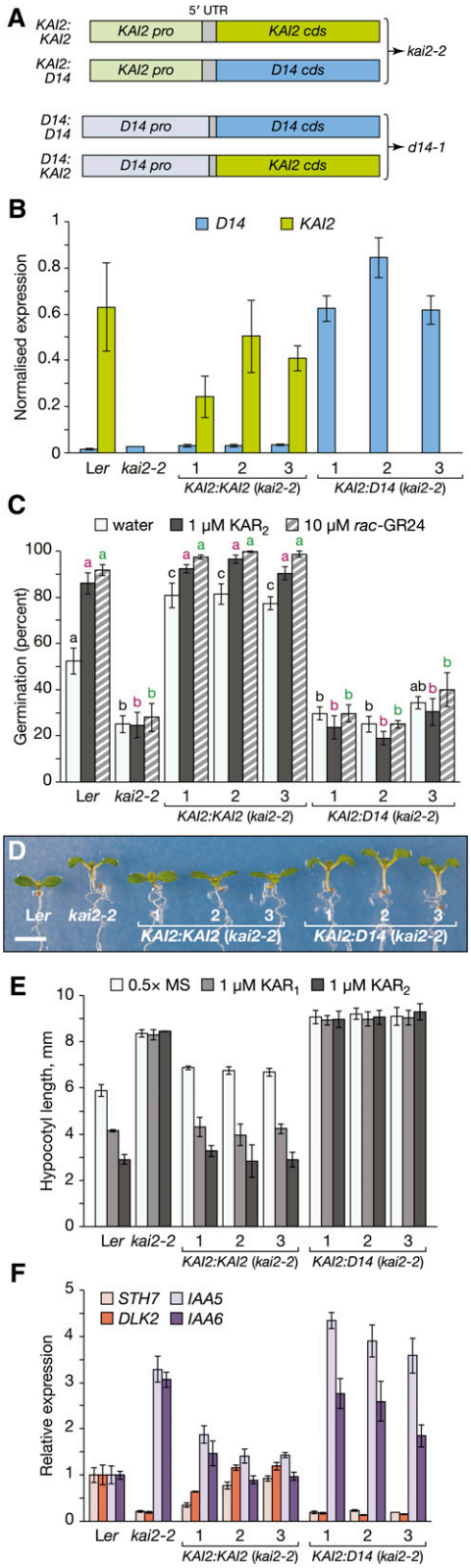


**Figure 1.** D14 Cannot Functionally Substitute for KAI2 in Regulating Arabidopsis Seed Germination and Seedling Morphogenesis.

2013). To investigate the role of the catalytic activity in KAI2 function, we generated stable transgenic *kai2-2* plants expressing mutant KAI2 protein in which the predicted catalytic serine residue was substituted with alanine (KAI2 S95A), expressed under the *KAI2* promoter (Waters et al., 2015). First, we examined the germination behavior of seed homozygous for the *KAI2 S95A* transgene. Three such lines showed no complementation of the *kai2-2* germination phenotype, with reduced germination rates relative to the wild type and no discernible response to $KAR_2$ or *rac*-GR24 (Figure 3A). In seedlings, *KAI2 S95A* was similarly unable to complement *kai2-2*, both in terms of overall seedling morphology (Figure 3B) and in terms of hypocotyl response to karrikins (Figure 3C). We also examined whether there was any detectable transcriptional response to $KAR_2$ in seedlings, in case small responses could not be detected by physiological assays. Levels of two karrikin-responsive and KAI2-dependent transcripts, *D14-LIKE2* (*DLK2*) and *INDOLE-3-ACETIC ACID INDUCIBLE6* (*IAA6*), showed no response to $KAR_2$ in *KAI2 S95A* seedlings, and they showed no consistent differences between *KAI2 S95A* and *kai2-2* (Figure 3D). To confirm that the S95A mutation did not negatively affect KAI2 protein stability, we generated an anti-KAI2 polyclonal antibody against a peptide epitope of Arabidopsis KAI2 that is on the surface of the protein and is predicted to have no cross-reactivity with related α/β-hydrolases (Supplemental Figures 2 to 4). The transgenic *KAI2 S95A* lines accumulated on average 3-fold more KAI2 protein than *KAI2pro:KAI2* transgenic controls, but only ~50% higher levels of *KAI2* transcripts (Figure 3E). Thus, the KAI2 S95A protein is stably expressed in seedlings.

**(A)** Strategy for validating *KAI2* and *D14* promoter activities and generating promoter swaps. DNA constructs were introduced into the indicated genetic backgrounds to generate stable transgenic lines. pro, promoter sequence; cds, protein coding sequence.

**(B)** Levels of *D14* and *KAI2* transcripts in imbibed seed of three independent homozygous lines carrying *KAI2pro:KAI2* or *D14pro:KAI2* transgenes in the *kai2-2* background.

**(C)** Germination responses to treatment with the germination stimulants $KAR_2$ and *rac*-GR24 of primary dormant Arabidopsis seed homozygous for *KAI2pro:KAI2* or *KAI2pro:D14* transgenes. Three independent transgenic lines were assayed; data are mean ± SE; $n = 3$ independent batches of seed per genotype, ≥75 seed per batch. Shared lowercase letters of the same color indicate no significant difference between genotypes within the same treatment group (ANOVA; $P < 0.05$).

**(D)** Representative homozygous *KAI2pro:KAI2* and *KAI2pro:D14* seedlings after 7 d growth on 0.5× MS medium in continuous white light. Bar = 2 mm.

**(E)** Hypocotyl elongation responses of homozygous *KAI2:KAI2* and *KAI2:D14* seedlings grown for 4 d under continuous red light on medium supplemented with $KAR_1$ or $KAR_2$. Data are means ± SE of $n = 3$ independent experiments, ≥20 seedlings per sample.

**(F)** Levels of KAI2-dependent marker transcripts *STH7*, *DLK2*, *IAA5*, and *IAA6* in *KAI2pro:KAI2* and *KAI2pro:D14* seedlings grown for 4 d under continuous red light on 0.5× MS medium. Transcripts were normalized to *CACS* reference transcripts and expressed relative to the value for untreated L*er* seedlings. Data are means ± SE of $n = 3$ biological replicates, ≥50 seedlings per sample.

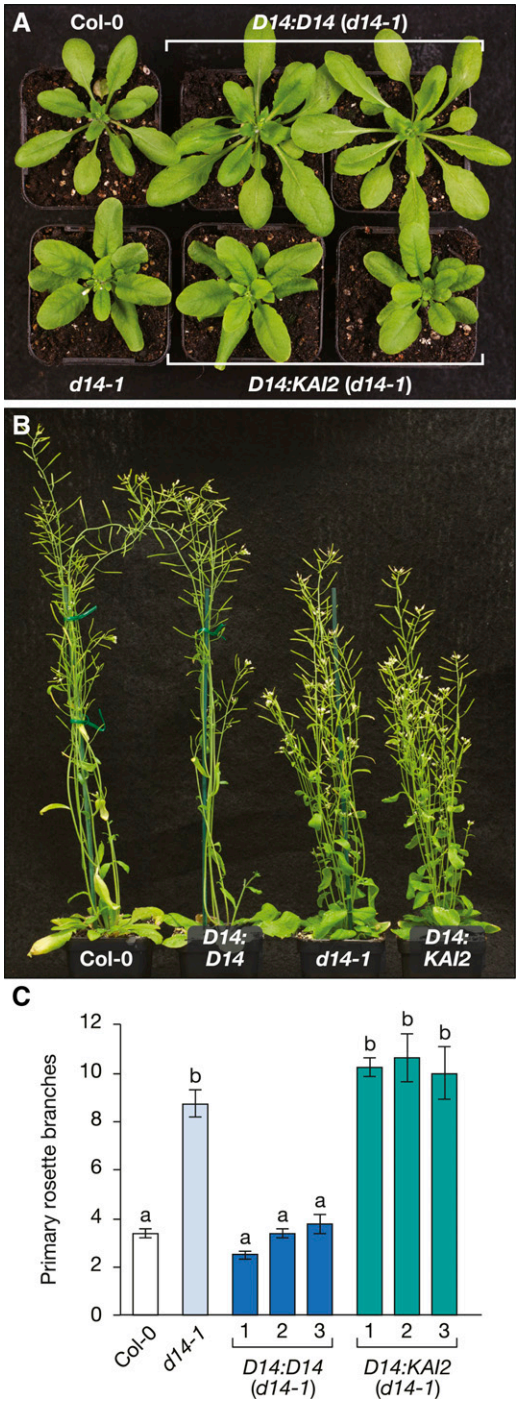


**Figure 2.** KAI2 Cannot Functionally Substitute for D14 in the Control of Leaf Growth and Shoot Branching.

**(A)** Rosette and leaf phenotypes of *D14pro:D14* and *D14pro:KAI2* plants grown under a 16-h-day/8-h-night cycle. Individuals of two independent transgenic lines are shown. Plants were photographed 30 dpg.
**(B)** Shoot branching phenotype of mature plants at 46 dpg.
**(C)** Primary rosette branch counts in three transgenic lines per construct at 51 dpg. Data are means ± SE of $n = 7$ to 8 plants per line. Lowercase letters indicate values that do not differ significantly (ANOVA, $P < 0.05$).

Together, these data demonstrate that the catalytic serine is necessary for these aspects of KAI2 function.

The *kai2-1* allele encodes a missense mutation that converts Gly-133 to glutamic acid (G133E). Gly-133 is located on a long, protruding loop that joins the α/β-fold hydrolase domain to the cap domain of KAI2 and related proteins (Supplemental Figure 1) (Hamiaux et al., 2012; Bythell-Douglas et al., 2013; Zhao et al., 2013). This residue is the first in a short GGF motif that is absolutely conserved among this family of α/β-fold hydrolases, from bacteria to plants (Supplemental Figure 2). *kai2-1* mutants have a strong phenotype with no detectable karrikin response (Waters et al., 2012a). It has been suggested that, because G133 is located on the external surface of the protein, the G133E mutation may result in impaired protein-protein interactions and thus render the protein inactive in downstream signal transduction (Kagiyama et al., 2013). However, using the α-KAI2 antibody, which recognizes an epitope independent of Gly-133, we observed no detectable protein in *kai2-1* lysates (Figure 3E). In addition, we have been unable to express KAI2 G133E in *Escherichia coli*, but we have expressed wild-type KAI2 and KAI2 S95A successfully (Supplemental Figure 5). Thus, we conclude that the evolutionarily conserved Gly-133 residue is essential for the function of KAI2 and related proteins mainly because it is required for protein tertiary structure and/or stability. Nevertheless, we do not exclude the possibility that this region of KAI2 is also required for downstream signaling.

### KAI2 Homologs from *M. polymorpha* and *S. moellendorffii* Exhibit Hydrolytic Activity and Substrate Selectivity

Having established functional differences between KAI2 and D14 proteins in Arabidopsis, we wondered when during plant evolutionary history these functions might have emerged. Previously, we identified two KAI2 homologs from *S. moellendorffii* (termed here Sm-KAI2a and Sm-KAI2b) and two from *M. polymorpha* (Mp-KAI2a and Mp-KAI2b) (Waters et al., 2012a). While phylogenetic analyses have grouped Sm-KAI2a, Mp-KAI2a, and Mp-KAI2b within the core KAI2 clade, Sm-KAI2b instead sits on a comparatively long branch that is a sister group to all D14 sequences from seed plants (Figure 4A) (Delaux et al., 2012; Waters et al., 2012a). As taxonomic sampling of sequences between seed plants and liverworts is sparse, the phylogenetic relationship of Sm-KAI2b relative to true D14 proteins is ambiguous (Figure 4A). To infer the function of these proteins, first we assessed their activity as hydrolytic enzymes. Functional enzymatic data on this family of proteins are limited, having been described only for angiosperm members. The petunia ortholog of D14, DAD2, hydrolyzes *rac*-GR24 in vitro, as do rice D14 and Arabidopsis D14 (Hamiaux et al., 2012; Zhao et al., 2013). A further report indicates that Os-D14 has a preference for the naturally configured 5DS enantiomer ($GR24^{5DS}$) over the non-natural $GR24^{ent\text{-}5DS}$ (Nakamura et al., 2013). Arabidopsis KAI2 (hereafter At-KAI2) meanwhile has been reported to have weak GR24 hydrolytic activity compared with Os-D14 and At-D14, but no information about enantiomer specificity was described (Zhao et al., 2013).

We expressed and purified Mp-KAI2b, Sm-KAI2a, and Sm-KAI2b proteins, alongside At-KAI2 and At-KAI2 S95A for

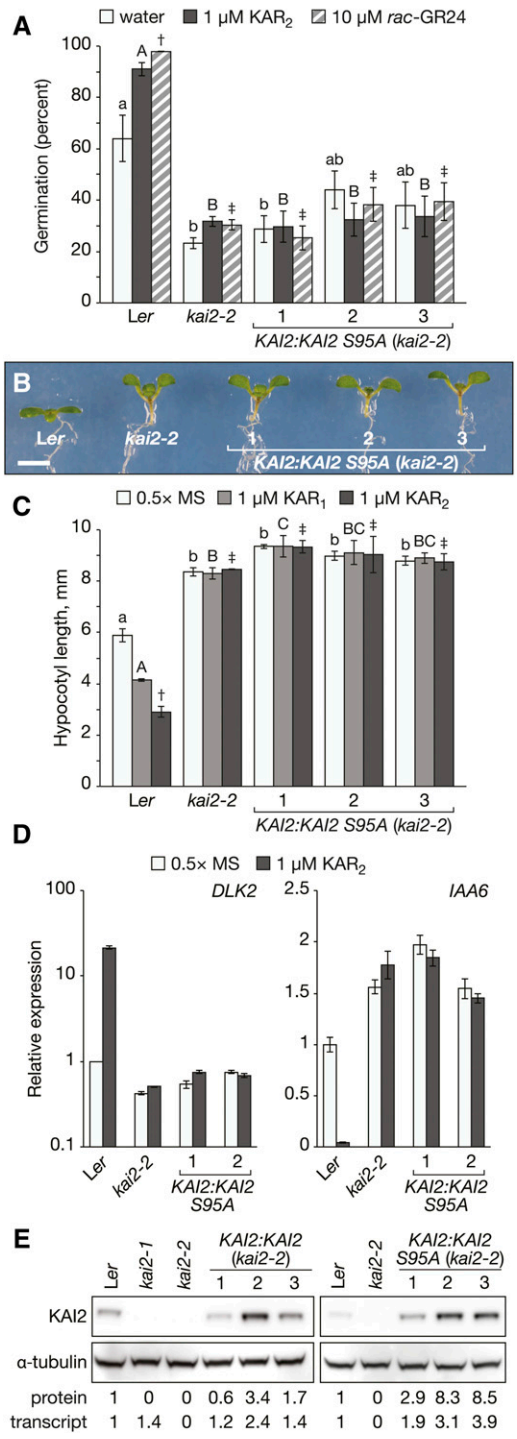


**Figure 3.** Evolutionarily Conserved Amino Acids Ser-95 and Gly-133 Are Essential for KAI2 Function in Arabidopsis.

**(A)** Germination responses of Arabidopsis seed expressing mutated KAI2 protein from the *KAI2* promoter in *kai2-2* (*KAI2:KAI2 S95A*). Three independent transgenic lines were assayed. Data are mean ± SE; $n = 3$ independent batches of seed per genotype, ≥75 seed per batch.

**(B)** Representative seedlings of each genotype after 7 d growth on 0.5× MS medium in continuous white light. Bar = 2 mm.

comparison (Supplemental Figure 4). Attempts to express Mp-KAI2a in *E. coli* were unsuccessful. First, we tested the activity of each protein toward *para*-nitrophenol acetate (*p*NPA), a generic substrate for esterases. With the exception of the AtKAI2 S95A mutant, all proteins exhibited hydrolytic activity toward *p*NPA in a substrate concentration-dependent manner consistent with Michaelis-Menten kinetics (Figure 4B). All three KAI2 proteins from *M. polymorpha* and *S. moellendorffii* exhibited higher maximum activity ($V_{max}$) than At-KAI2, but broadly similar affinity ($K_m$) toward the substrate (Supplemental Figure 6). Thus, Mp-KAI2b, Sm-KAI2a and Sm-KAI2b are all functional esterases, consistent with their identity as KAI2 homologs.

Next, we tested each protein for activity toward GR24. In Arabidopsis seedlings, $GR24^{5DS}$ acts mainly via At-D14, whereas $GR24^{ent\text{-}5DS}$ signals via At-KAI2, implying that At-D14 and At-KAI2 function depends in part on substrate stereochemistry (Scaffidi et al., 2014). Accordingly, we suspected that this characteristic might apply to other members of the same protein family, so we asked whether each protein might exhibit altered specificity toward different enantiomers of GR24. We monitored the hydrolytic activity of each enantiomer based on the consumption of substrate. At-KAI2 only showed activity toward $GR24^{ent\text{-}5DS}$, while At-KAI2 S95A was inactive against both enantiomers, consistent with the requirement of Ser-95 for biological activity (Figure 4C). Both Mp-KAI2b and Sm-KAI2b exhibited relatively strong hydrolytic activity upon different enantiomers, with the proteins favoring $GR24^{ent\text{-}5DS}$ and $GR24^{5DS}$, respectively (Figure 4C). Notably, Sm-KAI2b has activity consistent with that reported for Os-D14 (Nakamura et al., 2013). However, Sm-KAI2a had statistically negligible activity toward GR24 enantiomers in this hydrolysis assay, despite its clear activity as an esterase (Figures 4B and 4C).

Interaction between a ligand and a protein receptor can be inferred using differential scanning fluorimetry (DSF), in which the susceptibility of a protein to thermal denaturation is altered by the presence of a ligand that binds to the protein (Niesen et al., 2007). DSF has been used previously to infer interaction of *rac*-GR24 with both DAD2 and At-D14 (Hamiaux et al., 2012; Abe et al., 2014). Accordingly, we performed DSF assays to

**(C)** Hypocotyl elongation responses of KAI2 S95A seedlings grown on 0.5× MS medium supplemented with $KAR_1$ or $KAR_2$. Data are means ± SE of $n = 3$ independent experiments, ≥20 seedlings per sample.

**(D)** *DLK2* and *IAA6* transcript levels in seedlings grown on 0.5× MS medium with or without 1 μM $KAR_2$. Transcripts were normalized to *CACS* reference transcripts and expressed relative to the value for untreated L*er* seedlings. Data are means ± SE of $n = 3$ biological replicates, ≥50 seedlings per sample.

**(E)** Immunoblots of KAI2 and KAI2 S95A from 7-d-old seedlings. Left panels: L*er*, *kai2-1*, *kai2-2*, and three complementation lines expressing wild-type KAI2 from the *KAI2* promoter. Right panels: KAI2 S95A in three transgenic lines compared with wild-type KAI2 in L*er*. Protein and transcript levels were derived from the same material and are expressed relative to L*er*. Protein levels were normalized to α-tubulin and transcripts to *CACS*.

Shared lowercase letters, uppercase letters, or symbols indicate no significant difference between genotypes within the same treatment group (ANOVA, $P < 0.05$).

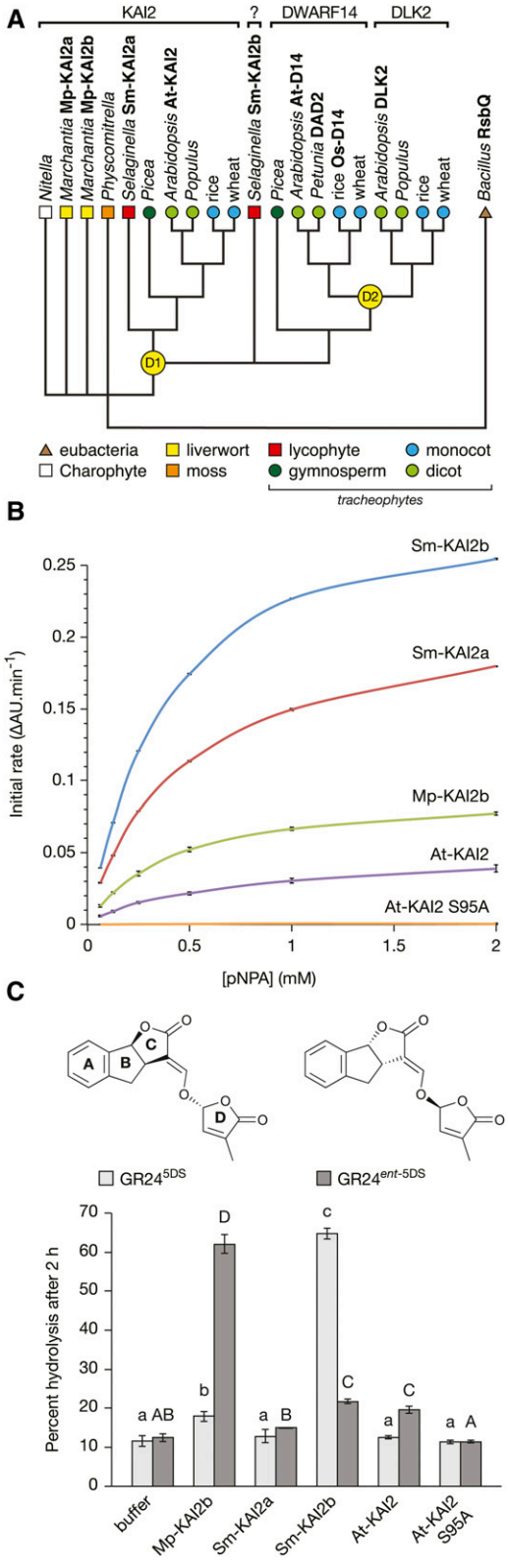


**Figure 4.** *M. polymorpha* and *S. moellendorffii* KAI2 Homologs Exhibit Generic Hydrolase Activity but Differential Activity toward Stereoisomers of GR24.

establish whether the observed hydrolytic activities of KAI2 homologs toward the two GR24 enantiomers correlated with a ligand-dependent shift in protein melting temperature. First, we found that the At-KAI2 melting temperature decreased and broadened in the presence of GR24$^{ent\text{-}5DS}$ at higher concentrations but was insensitive to GR24$^{5DS}$ at all concentrations tested (Figure 5). It is noteworthy that this specificity of At-KAI2 toward GR24$^{ent\text{-}5DS}$ is reflected in multiple physiological and molecular responses in planta (Scaffidi et al., 2014; Waters et al., 2015). As anticipated, the S95A mutation abolished the change in melting point of At-KAI2 in response to GR24$^{ent\text{-}5DS}$ (Figure 5). These results indicate that GR24$^{ent\text{-}5DS}$ interacts with At-KAI2, thus decreasing its thermal stability through ligand binding and/or hydrolysis, and that the catalytic serine is essential for this process. Mp-KAI2b showed a similar pattern to At-KAI2, responding only to higher concentrations of GR24$^{ent\text{-}5DS}$ (Figure 5). Sm-KAI2a, which showed negligible hydrolytic activity toward either GR24 enantiomer, likewise exhibited no change in melting temperature under the concentrations tested (Figure 5). Sm-KAI2b showed a strong response to all concentrations of GR24$^{5DS}$ and a weak response to 200 μM GR24$^{ent\text{-}5DS}$ (Figure 5), again consistent with the hydrolysis data described above. For comparison, we also examined the behavior of At-D14 in the same DSF assay. Surprisingly, we discovered that At-D14 responded to both enantiomers of GR24: Both induced a concentration-dependent shift between two discrete melting temperatures, suggestive of two distinct protein states (Figure 5). Furthermore, At-D14 was more responsive to GR24$^{ent\text{-}5DS}$ than GR24$^{5DS}$, with a change in melting temperature discernible at 10 and 50 μM, respectively. These changes were abolished in

**(A)** Simplified phylogeny of the KAI2 and D14 protein family. *M. polymorpha* and *S. moellendorffii* each possess two predicted KAI2 homologs. While Mp-KAI2a, Mp-KAI2b, and Sm-KAI2a belong unambiguously to the KAI2 clade, Sm-KAI2b does not, instead weakly grouping with D14 and DLK2 (D14-LIKE2) sequences from seed plants. This ambiguity in clade assignment is denoted with a question mark. For clarity, numerous KAI2 paralogs encoded by the *Physcomitrella* genome are omitted, but all group within the KAI2 clade. D1 and D2 indicate postulated gene duplication events. D1 is assumed to have happened prior to the emergence of tracheophytes, to give rise to Sm-KAI2a and Sm-KAI2b. D2 occurred after the split of gymnosperms and angiosperms to give rise to the angiosperm-specific DLK2 clade. Diagram is based upon phylogenetic data from Waters et al. (2012a) and Delaux et al. (2012), and modified, with permission, from Waters et al. (2013).

**(B)** Hydrolytic activity of Mp-KAI2b, Sm-KAI2a, Sm-KAI2b, At-KAI2, and At-KAI2 S95A SUMO fusion proteins toward the generic, chromogenic hydrolase substrate *p*NPA. Each data point is the mean ± SD of three technical replicates.

**(C)** Mp-KAI2b, Sm-KAI2a, Sm-KAI2b, At-KAI2, and At-KAI2 S95A SUMO fusion proteins were incubated with one of the two enantiomers of GR24 (GR24$^{5DS}$ and GR24$^{ent\text{-}5DS}$) as substrates. Hydrolysis of GR24 was monitored by HPLC after 2 h of incubation at 22°C. Data are expressed as percentage of substrate hydrolyzed. Note that there is chemical hydrolysis of GR24 in buffer alone. Data are means ± SD of $n$ = 3 independent hydrolysis reactions. Shared letters of the same case indicate no significant difference in activity upon the same substrate (ANOVA, $P < 0.05$).

the At-D14 S97A mutant (Supplemental Figure 7), as has been observed previously for *rac*-GR24 (Hamiaux et al., 2012; Abe et al., 2014). Consistent with the DSF data, we found that At-D14 hydrolyzed both GR24 enantiomers and indeed favored $GR24^{ent\text{-}5DS}$ over $GR24^{5DS}$ (Supplemental Figure 7). Overall, the DSF data and the GR24 hydrolysis data are mutually consistent and suggest that enantiomer-specific substrate hydrolysis is associated with a protein conformational change. It is also clear that different homologous proteins exhibit distinct responses to the same ligand, which potentially might reflect protein activity in planta.

Having established that DSF assays reflect the biochemical activity of KAI2 and D14 proteins toward GR24, we reasoned that karrikins might also induce a change in At-KAI2 melting temperature. However, we found that even at 200 μM, which is a 10-fold molar excess of ligand over protein, neither $KAR_1$ nor $KAR_2$ had any apparent effect on the melting temperatures of wild-type At-KAI2 or At-KAI2 S95A (Supplemental Figure 8). As expected, karrikins also had no effect on At-D14 melting temperature, consistent with the observation that At-D14 responds specifically to SL analogs (Supplemental Figure 8). Given that $KAR_2$ is generally more active than $GR24^{ent\text{-}5DS}$ in many KAI2-dependent responses, the lack of response of At-KAI2 to karrikins was surprising and indicates that the molecular interaction of karrikins and $GR24^{ent\text{-}5DS}$ with KAI2 may differ in important details.

### Sm-KAI2a and Sm-KAI2b Exhibit Differential Activity in Arabidopsis

To investigate whether the biochemical function of KAI2 homologs from non-seed plants is consistent with KAI2 and/or D14 function in Arabidopsis, we adopted a genetic complementation approach using the previously validated Arabidopsis *KAI2* and *D14* promoter sequences to drive heterologous expression in *kai2-2* and *d14-1* mutants.

First, we examined the ability of *KAI2pro:*Sm-*KAI2a* and *KAI2pro:*Sm-*KAI2b* transgenes to complement the *kai2-2* phenotype. In seed germination assays, neither transgene could restore germination levels to that of L*er* controls and neither had a significant effect upon germination levels in response to $KAR_2$ or *rac*-GR24 (Figure 6A). In seedlings, however, the hypocotyl length and cotyledon morphology of three independent lines expressing *KAI2pro:*Sm-*KAI2a* were intermediate between that of L*er* and *kai2-2*, demonstrating partial complementation of the *kai2-2* phenotype (Figure 6B). In comparison, three *KAI2pro:*Sm-*KAI2b* lines were morphologically indistinguishable from *kai2-2* (Figure 6B). In hypocotyl elongation assays, mock-treated *KAI2pro:*Sm-*KAI2a* seedlings again were intermediate relative to L*er* and *kai2-2* and did not show any response to either $KAR_1$ or $KAR_2$ (Figure 6C).The *KAI2pro:*Sm-*KAI2b* lines were identical to *kai2-2* seedlings and did not show any response to either $KAR_1$ or $KAR_2$ (Figure 6C). We examined *DLK2* and *IAA5* transcript levels in seedlings, and while both *DLK2* and *IAA5* showed partial restoration toward wild-type levels in untreated *KAI2pro:*Sm-*KAI2a* seedlings, there was no discernible response to $KAR_2$ (Figure 6D). Surprisingly, *DLK2* and *IAA5* transcript levels were only marginally different between *KAI2pro:*Sm-*KAI2a* and *KAI2pro:*Sm-*KAI2b* seedlings, despite the clear difference in morphology (Figures 6B and 6D). Nevertheless, while expression of Sm-KAI2a or Sm-KAI2b is insufficient to complement fully the phenotype of *kai2-2* during seed germination and seedling development, Sm-KAI2a can partially substitute for At-KAI2 function in seedlings. Most importantly, Sm-KAI2a does not mediate a karrikin response, suggesting that Sm-KAI2a does not perceive karrikins as a signaling ligand but can perceive an At-KAI2-dependent signaling compound that is present in Arabidopsis. Testing the ability of Sm-KAI2a to mediate responses to SL analogs was not feasible at this stage because these seedlings contain a functional At-D14.

These results allowed us to infer that, like in Arabidopsis, there might be a functional distinction between two KAI2 homologs in *S. moellendorffii*. Therefore, we next considered whether either Sm-*KAI2a* or Sm-*KAI2b* could mediate shoot responses to SLs by expressing the two coding sequences under control of the Arabidopsis *D14* promoter and in the *d14-1* background. However, neither transgene could discernibly complement the dwarfism or increased shoot branching phenotype of *d14-1* (Figures 6E and 6F). This finding implies that both *S. moellendorffii* KAI2 homologs are functionally distinct from At-D14, despite the biochemical activity of Sm-KAI2b toward GR24 with SL-like stereochemistry.

To test the functionality of the two *M. polymorpha* KAI2 homologs within Arabidopsis, we performed a similar set of transgenic experiments. Neither *KAI2pro:*Mp-*KAI2a* nor *KAI2pro:*Mp-*KAI2b* could rescue the overall seedling phenotype of *kai2-2* and neither could confer karrikin responses upon seedlings in hypocotyl elongation assays (Supplemental Figures 9A and 9B). Similarly, neither transgene could complement the dwarfism or increased shoot branching phenotype of *d14-1* (Supplemental Figures 9C and 9D). These findings indicate that the additional evolutionary time between *M. polymorpha* and *S. moellendorffii* relative to Arabidopsis has led to substantial functional divergence in KAI2 homologs, such that any conservation in function, within plants at least, can no longer be detected.

### Sm-KAI2a Is Functionally Equivalent to At-KAI2 in Adult Arabidopsis Tissue

The *kai2* phenotype extends beyond seedling development and into the adult phase. Rosette leaves adopt an elongated, narrowed profile in which the transition from petiole to leaf blade is exaggerated, giving the rosette a more spindly appearance (Figure 7A). In these respects, we noticed that *KAI2pro:*Sm-*KAI2a* plants resembled L*er*, but *KAI2pro:*Sm-*KAI2b* plants did not (Figure 7A). To assess this observation more precisely, we used LeafAnalyser software (Weight et al., 2008) to generate average leaf shape models derived from nodes 4 to 6 of multiple plants for each genotype (Figure 7B). To quantify the degree to which leaf morphology was altered by transgene expression, we determined the leaf midpoint ratio, which describes the distance of the widest point of the leaf relative to its overall length. Consistent with an elongated petiole, the widest point of *kai2* leaves shifted apically, and this shape was not modified significantly in plants expressing either *KAI2pro:*Sm-*SmKAI2b* or the

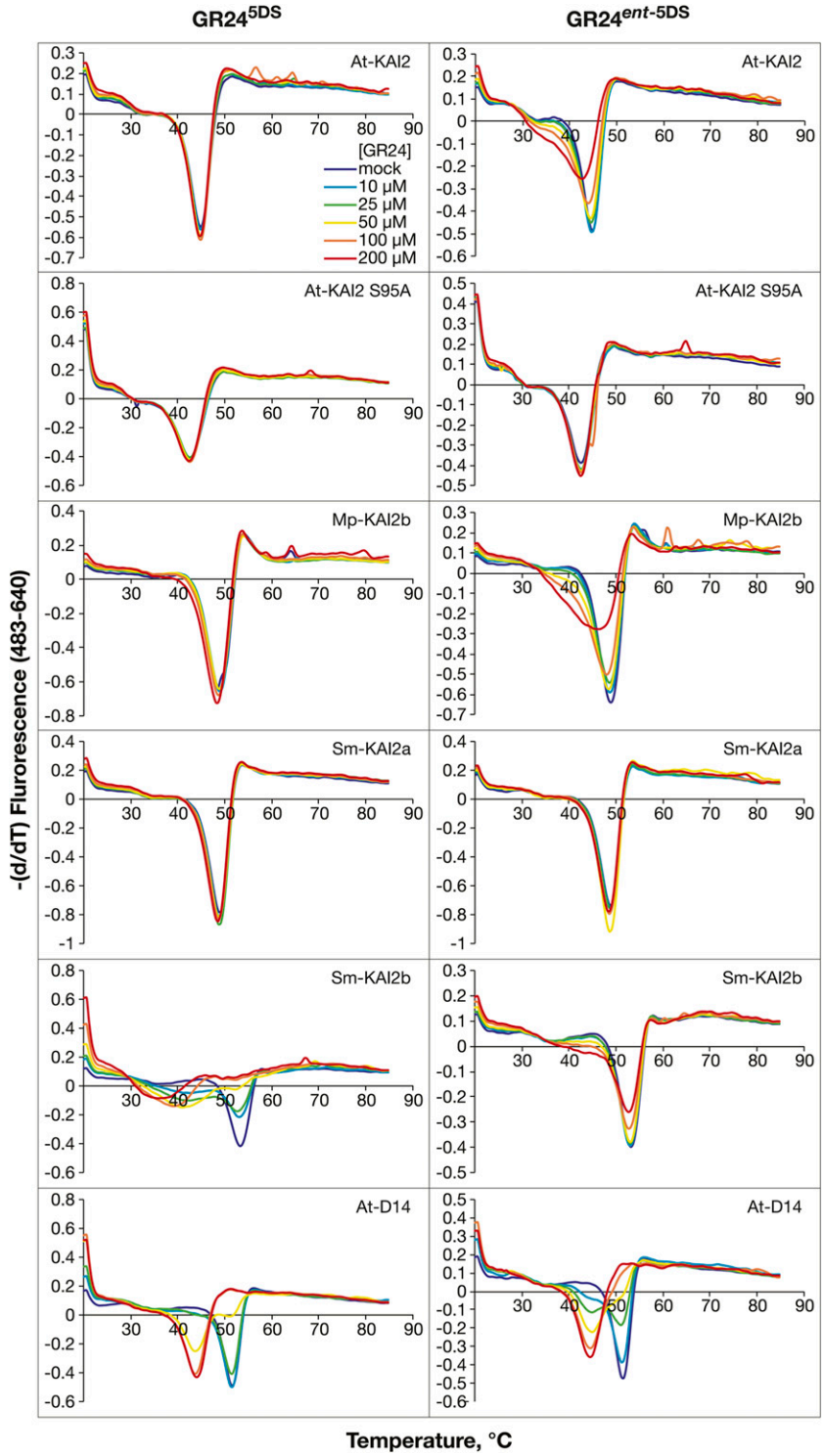


**Figure 5.** Responses of KAI2 Homologs to Enantiomers of GR24 as Determined by Differential Scanning Fluorimetry.

Purified SUMO fusion proteins were incubated with a fluorescent dye and increasing concentrations of the two enantiomers of GR24. The mixtures were heated gradually to induce protein melting, and the first derivative of the change in fluorescence was plotted against temperature. The inflection point or inverse peak of the curve was inferred to be the protein melting temperature. A shift in the melting point or shape of the curve suggests a protein-ligand interaction. Each line represents the average protein melt curve for four replicate samples run in parallel.

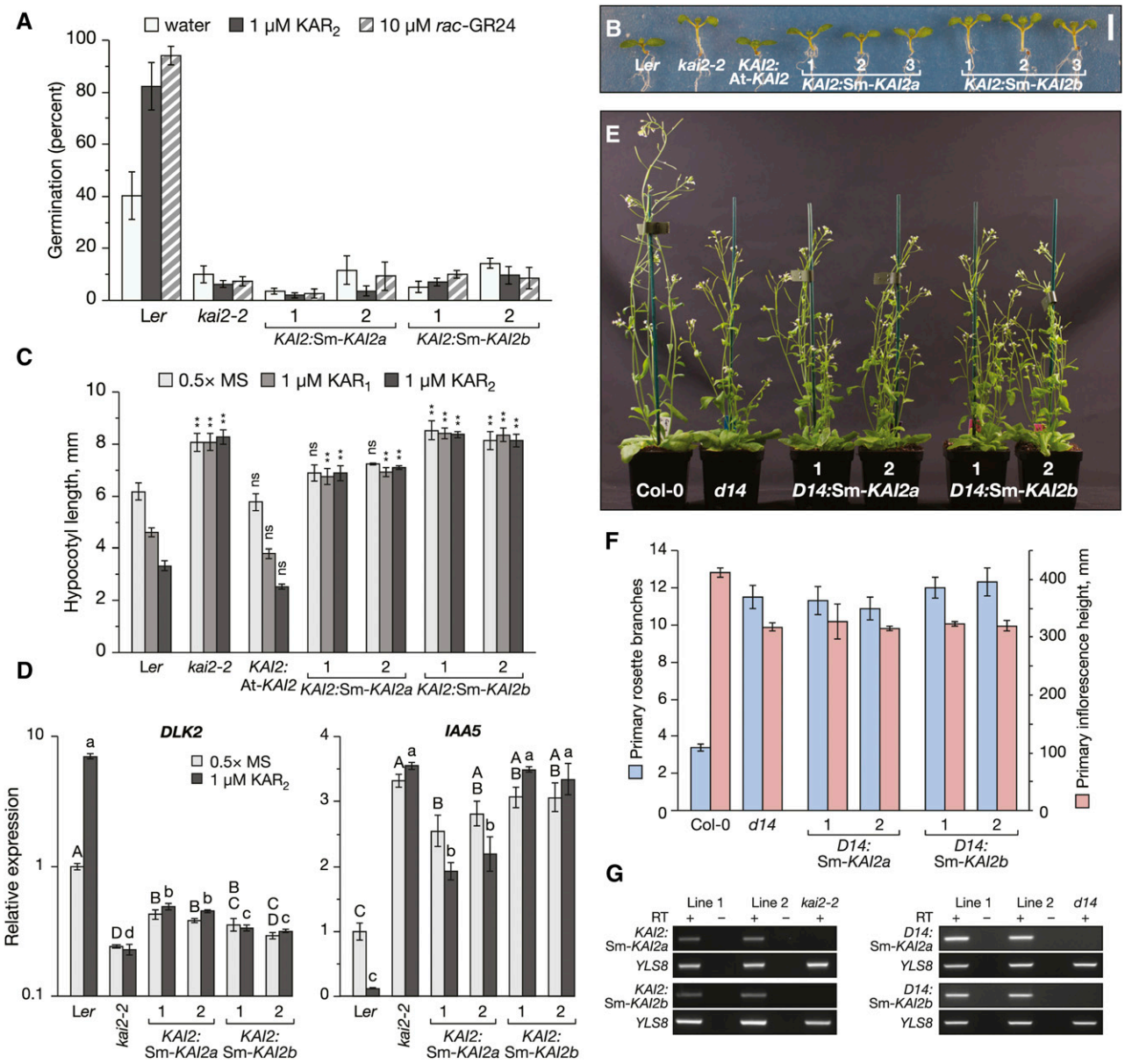


**Figure 6.** A KAI2 Homolog from *S. moellendorffii* Can Partially Complement the *kai2-2* Seedling Phenotype but Not *d14-1* Shoot Branching

**(A)** Germination responses of primary dormant Arabidopsis seed homozygous for *KAI2pro:*Sm-*KAI2a* or *KAI2pro:*Sm-*KAI2b* transgenes (in *kai2-2* background). Two independent transgenic lines were assayed. Data are mean ± SE; *n* = 3 independent batches of seed per genotype, ≥75 seed per batch.

**(B)** Representative seedlings of each genotype after 7 d growth in continuous white light. Three independent transgenic lines per construct are shown. Bar = 2 mm.

**(C)** Hypocotyl growth responses of independent transgenic lines homozygous for *KAI2pro:*Sm-*KAI2a* or *KAI2pro:*Sm-*KAI2b* compared with L*er*, *kai2-2*, and *KAI2:*At-*KAI2* seedlings grown for 4 d under continuous red light. Data are means ± SE of *n* = 3 to 5 independent experiments, with ≥20 seedlings per sample. Asterisks denote a significant difference from L*er* under the same treatment (ANOVA, $P < 0.01$); ns, not significant.

**(D)** Levels of *DLK2* and *IAA5* transcripts in seedlings expressing *KAI2pro:*Sm-*KAI2a* or *KAI2pro:*Sm-*KAI2b* grown for 4 d under continuous red light. Transcripts were normalized to *CACS* and expressed as fold change relative to L*er* grown on nonsupplemented 0.5× MS medium. Data are means ± SE (*n* = 3 biological replicates of >100 seedlings). Values with shared letters of the same case are not significantly different from one another (ANOVA, $P < 0.05$).

**(E)** Phenotype of plants expressing Sm-KAI2a and Sm-KAI2b from the Arabidopsis *D14* promoter, grown under a 16-h-day/8-h-night cycle at 37 dpg. Individuals of two independent transgenic lines are shown.

**(F)** Primary rosette branch count and primary inflorescence height of genotypes shown in **(D)**. Data are means ± SE of *n* = 7 to 8 plants per line.

nonfunctional *KAI2pro:*At-*KAI2 S95A* (Figures 7B and 7C). By contrast, the leaf midpoint ratio in *KAI2pro:*Sm-*KAI2a* plants was no different from that in L*er* or *KAI2pro:*At-*KAI2* transgenic control plants (Figures 7B and 7C). We then examined whether changes in gene expression might mirror the morphological complementation of *kai2-2* by Sm-*KAI2a*. In adult rosette leaves, as in seedlings, *kai2-2* mutants underexpress *STH7* and *KUF1* transcripts. These defects were restored by expression of *KAI2pro:*At-*KAI2*, but not by *KAI2pro:*At-*KAI2 S95A*, providing suitable baselines for comparisons with the other transgenic lines (Figure 7D). Unexpectedly, *KAI2pro:*At-*KAI2* plants showed an overcompensation of *STH7* expression relative to L*er*. Nevertheless, *KAI2pro:*Sm-*KAI2a* plants displayed a *STH7* transcript profile no different from *KAI2pro:*At-*KAI2*, and expression of *KUF1* was essentially restored to the wild type (Figure 7D). Notably, however, *KAI2pro:*Sm-*KAI2b* plants closely resembled *kai2-2* and *KAI2pro:*At-*KAI2 S95A* plants in these respects. In summary, these data demonstrate that Sm-KAI2a and Sm-KAI2b are functionally distinct and that Sm-KAI2a is functionally similar to At-KAI2 during the adult vegetative growth phase.

We considered that the failure of Sm-KAI2a to transduce a karrikin response in seedlings might be because the functional complementation of *kai2* is incomplete at this developmental stage (Figure 6). We therefore examined karrikin responses in older plants in which the *kai2* phenotype is more fully restored by Sm-KAI2a. We treated 17-d-old seedlings with 5 μM $KAR_2$ for 24 h in liquid culture and assessed transcriptional responses. Under these conditions, *STH7*, *IAA5*, and *IAA6* transcripts did not exhibit substantial changes in response to $KAR_2$, but *KUF1* and *DLK2* transcripts both increased strongly in *KAI2pro:*At-*KAI2* transgenic controls (Figure 7E). Surprisingly, $KAR_2$ treatment increased levels of *DLK2* transcripts ~2-fold in *kai2-2* mutants; this may represent a nonspecific effect of applying relatively high concentrations of $KAR_2$ at this developmental stage, but the change is small compared with the 50-fold increase observed in *KAI2pro:*At-*KAI2* plants. Regardless of the basis for this discrepancy, *KUF1* and *DLK2* transcripts in *KAI2pro:*Sm-*KAI2a* transgenics did not show any response to $KAR_2$ over and above that observed in *kai2*. Therefore, we conclude that Sm-KAI2a cannot mediate responses to karrikins, regardless of developmental context.

### Sm-KAI2a Cannot Transduce Signals from SL Analogs or Carlactone

Despite the negligible enzymatic activity of Sm-KAI2a toward GR24 in vitro, we sought to ascertain whether Sm-KAI2a could mediate signals from GR24 in planta, as is the case for At-KAI2. We crossed both *KAI2pro:*Sm-*KAI2a* transgenic lines with the *d14 kai2* double mutant to remove endogenous D14 function, which would otherwise confound Sm-KAI2a-mediated responses to GR24. Based on hypocotyl elongation assays, Sm-KAI2a was unable to confer plant responses to GR24, either as individual enantiomers or as a racemic mixture (Figure 8A). We also tested a racemic mixture of CN-debranone, which is a highly active SL analog that can signal via both At-KAI2 and D14 in L*er* (Fukui et al., 2011; Waters et al., 2012b; Scaffidi et al., 2014); however, this compound was also inactive in Sm-KAI2a transgenics (Figure 8A). Finally, we considered the possibility that Sm-KAI2a might perceive a product of the carlactone pathway, such as an endogenous SL. Carlactone does not promote a strong hypocotyl growth inhibition response in Arabidopsis but does induce transcriptional changes in several genes, mostly in a D14-dependent manner (Scaffidi et al., 2014). While L*er* seedlings responded clearly to both 10 μM *Z*-carlactone and 1 μM *rac*-GR24 in terms of *STH7*, *KUF1*, *DLK2*, and *IAA5* transcripts, two independent lines expressing Sm-KAI2a in the *d14 kai2* background were insensitive to both substances in this regard (Figure 8B). Overall, these data indicate that Sm-KAI2a cannot transduce signals from strigolactone analogs or carlactone derivatives, at least in the context of seedling development. Consistent with the inability of Sm-KAI2a to complement the *d14* phenotype, we conclude that that Sm-KAI2a is not a viable SL receptor, but instead shares overlapping functions with At-KAI2.

### The Catalytic Triad of SmKAI2a Is Essential for Function in Planta

The functional complementation of adult *kai2* phenotypes by Sm-KAI2a indicates that At-KAI2 and Sm-KAI2a are functionally similar. Moreover, the requirement for a functional catalytic triad in At-KAI2 suggests that hydrolytic activity, perhaps toward an endogenous butenolide ligand, is fundamental to At-KAI2-dependent signaling. However, as Sm-KAI2a does not confer responses to any of the tested butenolides, it is possible that Sm-KAI2a function in planta is independent of its demonstrated hydrolytic activity in vitro and, therefore, that Sm-KAI2a and At-KAI2 have different signaling mechanisms. To investigate this possibility, we generated a catalytic serine mutant (S94A) of Sm-KAI2a and expressed it in the Arabidopsis *kai2-2* background. To allow expression of Sm-KAI2a protein to be verified by immunoblot, we used a GFP tag and expressed the fusion protein under the same At-*KAI2* promoter as used in the previous experiments.

We introduced either a wild-type *KAI2pro:GFP*–Sm-*KAI2a* or mutated *KAI2pro:GFP*–Sm-*KAI2a S94A* transgene into the *kai2-2*

**Figure 6.** (continued).

**(G)** RT-PCR analysis of Sm-*KAI2a* and Sm-*KAI2b* transcripts. Left panels: expression in 4-d-old seedlings homozygous for *KAI2pro:*Sm-*KAI2a* or *KAI2pro:*Sm-*KAI2b*. Tissue was pooled from ~30 seedlings. Right panels: expression in the youngest rosette leaves (at the base of the inflorescence stem) of 32-d-old plants homozygous for *D14pro:*Sm-*KAI2a* or *D14pro:*Sm-*KAI2b*. Tissue was pooled from three plants per genotype. *YLS8* reference transcripts serve as a PCR control. RT, reverse transcriptase.

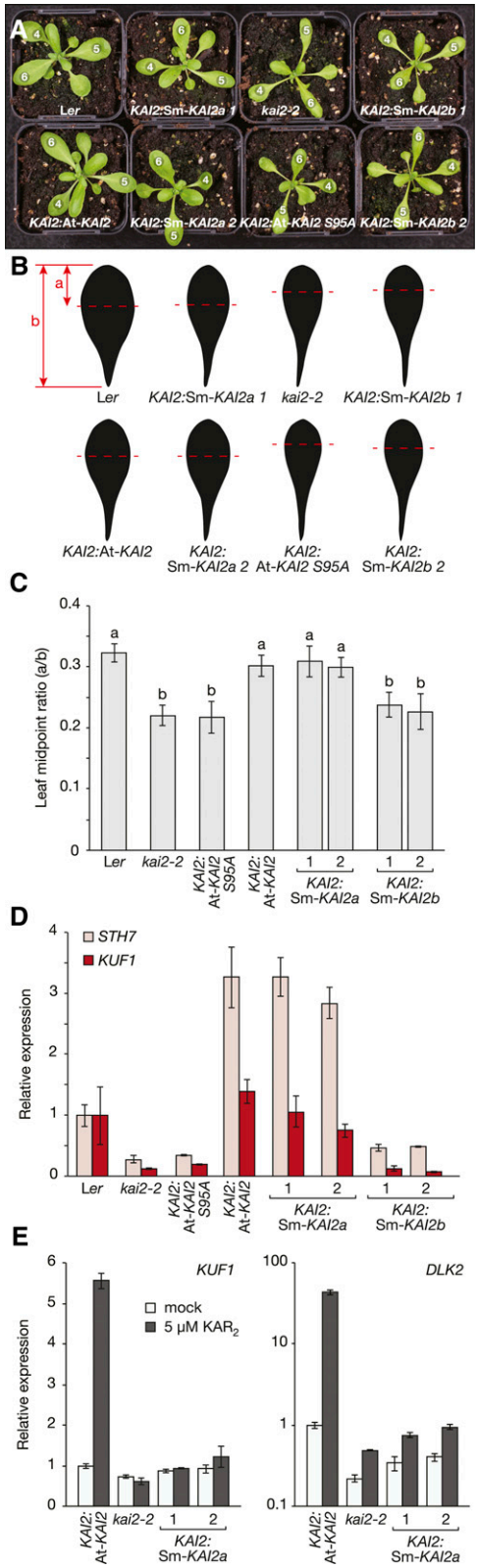


**Figure 7.** Adult *kai2-2* Phenotypes Are Complemented by Sm-*KAI2a* but Not Sm-*KAI2b*.

background and examined the resulting primary transformants. For the most appropriate comparisons, we used the *KAI2pro:*At-*KAI2* and *KAI2pro:*At-*KAI2 S95A* transgenics characterized previously (Figure 7). Of 14 recovered primary transformants expressing *KAI2pro:GFP*–Sm-*KAI2a*, 13 exhibited a wild-type leaf phenotype indistinguishable from that of *KAI2pro:*At-*KAI2* plants, results for six of which are presented here (Figure 9A), demonstrating that addition of GFP did not negatively impact Sm-KAI2a function. By contrast, all 12 primary transformants carrying *KAI2pro:GFP*–Sm-*KAI2a S94A* had leaf and rosette phenotypes similar to *KAI2pro:*At-*KAI2 S95A* plants, results for six of which are presented here (Figure 9B). The six primary transformants for each transgene were analyzed further by immunoblot and quantitative RT-PCR. While expression levels of the fusion proteins varied between individual plants, expression of both wild-type and mutated GFP–Sm-KAI2a proteins could be easily detected in leaves of at least four of the six primary transformants (Figure 9C). Importantly, this result indicates that the mutated Sm-KAI2a S94A protein is stable, as is Arabidopsis At-KAI2 S95A.

Finally, we analyzed levels of *STH7* and *KUF1* transcripts in the same tissue samples analyzed by immunoblot. Without exception, *KAI2pro:GFP*–Sm-*KAI2a* transformants had transcript levels similar to *KAI2pro:*At-*KAI2* plants, whereas *KAI2pro:GFP*–Sm-*KAI2a S94A* transformants resembled *KAI2pro:*At-*KAI2 S95A* plants in this respect (Figure 9D). Accordingly, we conclude that the function of Sm-KAI2a in planta is fully dependent on its catalytic serine; therefore, the activity of both Sm-KAI2a and At-KAI2 likely involves binding of an endogenous ligand that is susceptible to hydrolytic attack.

**(A)** Rosette and leaf morphology of plants homozygous for *KAI2pro:*At-*KAI2*, *KAI2pro:*At-*KAI2 S95A*, *KAI2pro:*Sm-*KAI2a*, or *KAI2pro:*Sm-*KAI2b* transgenes. Circled numbers denote leaf number, with the first true leaf defined as 1. For *KAI2pro:*Sm-*KAI2a* and *KAI2pro:*Sm-*KAI2b*, two independent transgenic lines were analyzed. Plants were grown under 16-h-day/8-h-night cycle and photographed at 21 dpg.

**(B)** Average leaf shape models produced by LeafAnalyser and derived from leaves 4 to 6 of the genotypes shown in **(A)**. Leaf models were calculated from seven plants per genotype and scaled to the length of L*er*. Red lines indicate the leaf midpoint, defined as the widest part of the leaf lamina, which is used to define the leaf midpoint ratio.

**(C)** Quantification of leaf midpoint ratio across leaves 4, 5, and 6. Data are means ± SD of $n = 7$ plants. Shared lowercase letters indicate no significant difference (ANOVA, $P < 0.01$).

**(D)** Levels of KAI2-dependent marker transcripts *STH7* and *KUF1* in leaves 4, 5, and 6. Tissue was pooled from 2 to 3 plants per genotype at 24 dpg, and data are means ± SE of $n = 3$ such pools. Transcripts were normalized to *TIP41L* reference transcripts and expressed relative to the value for L*er*.

**(E)** Responses of *KUF1* and *DLK2* transcripts in 15-d-old seedlings treated with 5 μM $KAR_2$ for 24 h in liquid culture. Data are means ± SE of $n = 3$ flasks of ~50 seedlings each. Transcripts were normalized to *TIP41L* and expressed relative to the value for mock-treated *KAI2pro:*At-*KAI2* seedlings.

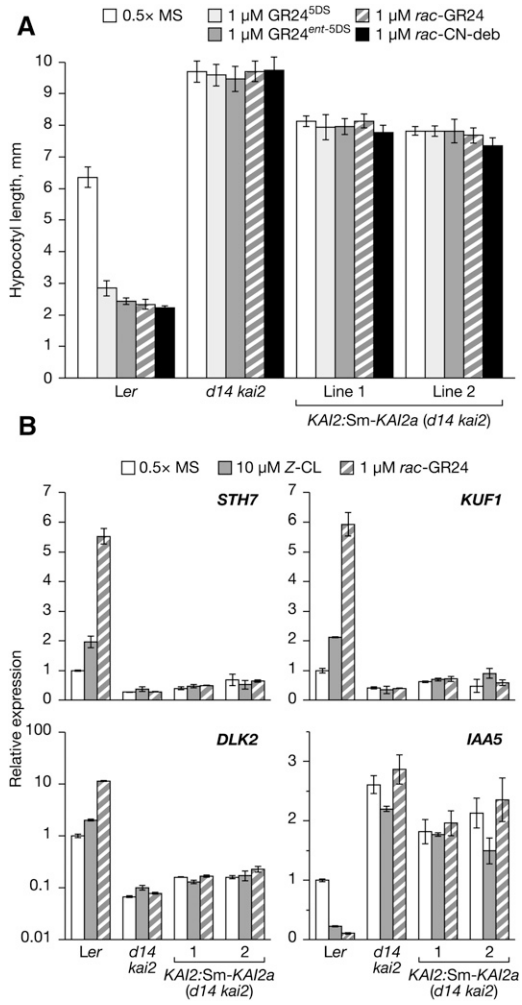


**Figure 8.** Sm-KAI2a Cannot Mediate Seedling Responses to Strigolactone Analogs or Carlactone.

**(A)** Hypocotyl elongation responses of seedlings expressing *KAI2pro:* Sm-*KAI2a* in an *d14 kai2* background to each GR24 enantiomer and to racemic CN-debranone, a strigolactone analog. Data are means ± SE of $n = 3$ independent experiments.

**(B)** Levels of *STH7*, *KUF1*, *DLK2*, and *IAA5* transcripts in seedlings treated with 10 μM *Z*-CL or 1 μM *rac*-GR24. Transcript levels were normalized to *CACS* and expressed as fold change relative to L*er* grown on nonsupplemented 0.5× MS medium. Data are means ± SE ($n = 2$ to 3 biological replicates of ~100 seedlings).

In both **(A)** and **(B)**, seedlings were grown for 4 d under continuous red light as described in Figure 1E.

## DISCUSSION

### Functional Distinctions between KAI2 and D14 in Arabidopsis

A function for KAI2 during plant development was inferred initially from its involvement in photomorphogenesis (Sun and Ni, 2011). The independent discovery of KAI2 as being essential for karrikin responses in Arabidopsis, and its close relationship with D14, have led to the general notion that KAI2 is a signaling component for butenolide compounds. In this study, we sought to understand more fully the mechanistic aspects of butenolide perception by KAI2 and to use functional complementation to analyze the evolutionary history of the KAI2/D14 family.

One explanation for the inability of natural SLs and GR24 isomers with naturally configured stereochemistry to stimulate seed germination in Arabidopsis might be the apparently low expression of D14 compared with KAI2 in seeds (Waters et al., 2012a; Scaffidi et al., 2014). If this were the sole explanation, then ectopic expression of D14 to KAI2-like levels in seed would restore sensitivity of *kai2* seed to *rac*-GR24, but it does not (Figure 2). This result reinforces the notion that endogenous canonical SLs do not have a major role in Arabidopsis seed germination. More importantly, it implies that activity is not only limited by ligand or receptor availability, but also by other factors such as SMAX1. Highly expressed in seed, *SMAX1* is epistatic to *MAX2* in the control of seed germination, with *smax1* mutations suppressing numerous seed-related phenotypes of *max2* (Stanga et al., 2013). Although not yet formally demonstrated, the relationship between KAI2 and MAX2 suggests that SMAX1 acts in the same pathway as KAI2 in the regulation of seed germination. The finding that ectopic expression of D14 confers neither normal seed germination levels nor responses to *rac*-GR24 upon *kai2* seed suggests that D14 cannot function with SMAX1. This inference would explain also why *smax1* cannot suppress the increased shoot branching phenotype of *max2* (Stanga et al., 2013), which is a D14-mediated trait. An analogous rationale could apply for the inability of KAI2 to mediate SL-dependent control of shoot branching (Figure 2): KAI2 may not function with the relevant SMXL family member(s), including presumably an Arabidopsis D53 ortholog. In this case, however, the lack of an appropriate ligand for KAI2 may also apply because KAI2 is a poor transducer of signals from natural SLs and carlactone (Scaffidi et al., 2013, 2014). Overall, KAI2 cannot be considered a receptor for carlactone-derived SLs in Arabidopsis, but instead is presumably a receptor for a non-carlactone-derived, butenolide compound active during seed germination and seedling establishment and throughout vegetative growth. In this vein, the ability of GR24 to affect seedling growth in an D14-dependent manner does not necessarily imply that endogenous SLs or D14 have a native biological function in Arabidopsis seedling growth, but instead suggests that D14 is merely capable of mediating responses when the appropriate exogenous ligands and protein partners are present. It is noteworthy that in rice seedlings, both D14 and KAI2 influence mesocotyl growth: While the D14-dependent response is mediated by canonical SLs, the signaling compound for the KAI2-dependent response is unknown (Kameoka and Kyozuka, 2015).

### Ligand-Receptor Mechanisms

Our results demonstrate that the catalytic serine of KAI2 is essential for both the endogenous functions of KAI2, regulating seed germination, seedling growth, and leaf morphology, and for mediating exogenous signals such as karrikins. The simplest interpretation of this finding is that bioactive ligands of KAI2 interact with the catalytic serine at some point in the signaling

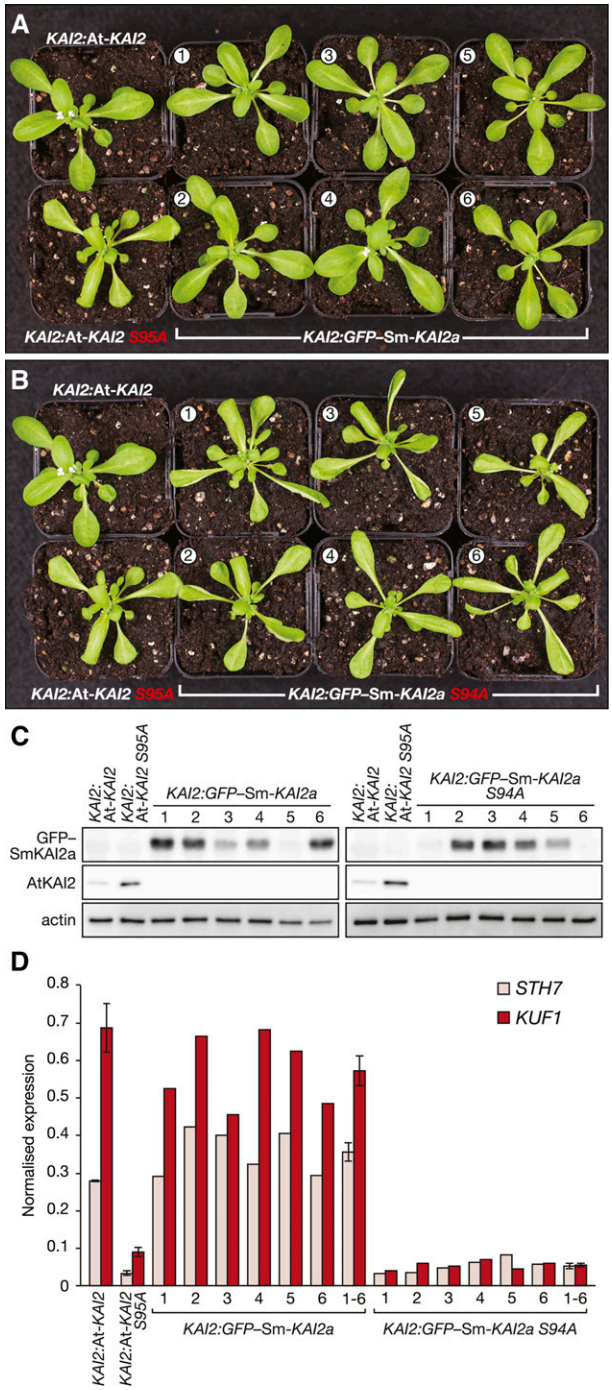


**Figure 9.** The Catalytic Serine of Sm-KAI2a Is Essential for Function in Arabidopsis.

**(A)** Phenotypes of six primary transformants (1 to 6) carrying a *KAI2pro:GFP–Sm-KAI2a* transgene in the *kai2-2* background, compared with *KAI2pro:*At-*KAI2* and *KAI2pro:*At-*KAI2 S95A* plants of the same age (31 d old).

**(B)** As for **(A)**, but the transgene confers a mutated catalytic serine in Sm-KAI2a (S94A).

**(C)** GFP-SmKAI2, At-KAI2, and actin levels from the plants depicted in **(A)** and **(B)**, determined by immunoblot.

process and that these ligands are susceptible to nucleophilic attack by the serine side chain. It is not yet clear whether the S95A mutation blocks KAI2 signaling because of a direct loss of ligand binding or because of a specific requirement for ligand hydrolysis. Nonetheless, the events associated with ligand binding and/or hydrolysis presumably trigger a change in protein state that constitutes a signal perceived by the cell.

In Arabidopsis, both karrikins and GR24$^{ent\text{-}5DS}$ evoke similar responses: They both stimulate seed germination, inhibit hypocotyl elongation, trigger similar transcriptional changes, and promote degradation of KAI2 protein (Scaffidi et al., 2014; Waters et al., 2015). However, our DSF data indicate that the molecular events occurring between each ligand and KAI2 must be distinct because karrikins do not induce a change in KAI2 melting temperature but GR24$^{ent\text{-}5DS}$ does. The reason for these distinct responses is not yet evident, but there are several possibilities. One is that the large change in thermal stability detected by DSF assays results not from ligand binding, but from ligand hydrolysis, which may be chemically unfavorable for karrikins. Perhaps ligand binding is key, and this binding induces a much smaller change in the state of KAI2 that is not readily detectable by DSF. A second possibility is that karrikins induce a change in state that is similar to that produced by GR24$^{ent\text{-}5DS}$ but, because karrikins may not be readily hydrolyzed, they only interact transiently with the active site, and the protein quickly relaxes back into the ligand-free state: This is the state detected by DSF. A third explanation is that $KAR_1$ and $KAR_2$ themselves are not direct substrates for KAI2, but instead are metabolically converted in planta into an active ligand that does induce the change in state responsible for signaling. Distinguishing between these possibilities will require substantial further work and will be assisted by crystal structures of KAI2 and D14 variants, particularly active site mutants, in ligand-bound and ligand-free states. Clearly, the central issue is deciphering the causal relationships between the events of ligand recognition, ligand hydrolysis, and signal transduction.

It was also surprising that At-D14 was active toward the non-natural GR24$^{ent\text{-}5DS}$ (2′*S*-configured) isomer and, indeed, more so than toward GR24$^{5DS}$ (2′*R*-configured). This preference is opposite to that described for Os-D14 (Nakamura et al., 2013). In physiological assays in Arabidopsis, it is clear that 2′*R* strigolactones are predominantly active through D14, although 2′*S* isomers retain some activity with respect to shoot branching control (Scaffidi et al., 2014). Therefore, biochemical activity does not necessarily predict biological activity: Arguably, ligand hydrolysis and a large change in protein state per se are insufficient to confer biological activity. It is possible that the two GR24 enantiomers induce different conformational changes in the protein, and these changes are recognized differentially by

**(D)** *STH7* and *KUF1* transcript levels in plants depicted in **(A)** and **(B)**. For *KAI2pro:*At-*KAI2* and *KAI2pro:*At-*KAI2 S95A* controls, three plants were analyzed per genotype (data are mean ± SE). For the *KAI2pro:GFP–SmKAI2a* and *KAI2pro:GFP–SmKAI2a S94A* primary transformants, expression levels in each individual plant are shown, together with the mean ± SE of all six (1 to 6). Transcript levels are normalized to *TIP41L* transcripts.

signaling partners. Alternatively, as speculated above, the large change in protein thermal stability detected by DSF is a specific result of the process of hydrolysis and is not necessarily the signal perceived by signaling partners.

Recently, it was shown that D14 is destabilized and degraded in a MAX2-dependent manner following the addition of exogenous *rac*-GR24 (Chevalier et al., 2014). A similar process occurs for Arabidopsis KAI2 upon karrikin signaling, although this degradation is independent of MAX2. Importantly, ligand-dependent degradation of KAI2 occurs subsequent to signaling because the KAI2 S95A mutant is resistant to such degradation (Waters et al., 2015). If the changes in protein state associated with ligand binding and/or hydrolysis were irreversible, then the degradation process would serve to remove the activated receptor after signaling.

### Evolution of KAI2 and D14

From our transgenic cross-species complementation experiments, we can draw four primary conclusions: (1) Esterase activity is necessary, but not sufficient for KAI2 function in plants. (2) Among the two *S. moellendorffii* KAI2 homologs, only Sm-KAI2a has KAI2 function similar to that in Arabidopsis. (3) Neither *S. moellendorffii* KAI2 homolog has D14 function similar to that in Arabidopsis. (4) Neither *M. polymorpha* KAI2 homolog has either KAI2 or D14 function in Arabidopsis. The ability of Sm-KAI2a to complement the Arabidopsis *kai2* mutant, but not *d14*, is consistent with KAI2 being functionally more ancient than D14. Logically, therefore, the KAI2-dependent signaling pathway must predate D14-dependent SL signaling and suggests that the latter evolved from the former. Furthermore, substantial similarity in the KAI2 signal transduction pathway must exist between *S. moellendorffii* and Arabidopsis, indicating that this developmental mechanism was present in the ancestor of vascular plants some 400 million years ago. By contrast, D14-mediated control of shoot branching appears to be a relatively recent innovation that coincided with the arrival of seed plants.

It is particularly curious that Sm-KAI2a cannot substitute for At-KAI2 function in seed, can do so partially in seedlings, and is essentially fully functional in adult plants. This gradual transition might reflect developmental phases that are simply not present in *S. moellendorffii*: While the iterative, vegetative growth phase of the *S. moellendorffii* sporophyte and Arabidopsis rosette can be broadly considered homologous, there is no close *S. moellendorffii* equivalent to the seed. Conceptually, the seedling is an establishment phase of the young sporophyte, so an intermediate degree of functional similarity between the two plants might be expected. A straightforward hypothesis might be that the recent "seed" SMXL family members cannot function with Sm-KAI2a, but the more evolutionarily ancient "vegetative" members can. Considering that KAI2 function is essentially conserved, it will be most interesting to examine whether evolutionary diversification of the SMXL family can account for the varied ability of Sm-KAI2a to function in Arabidopsis. Although a more thorough phylogenetic analysis is required, members of the D53 and SMAX1 clades have not been identified in non-vascular plants, but *P. patens* does have three members of the broader SMXL family (Zhou et al., 2013).

Despite the broad conservation of function with At-KAI2, Sm-KAI2a was unable to confer responses upon Arabidopsis to any of the tested exogenous ligands: karrikins, debranones, GR24, or carlactone. Sm-KAI2a can hydrolyze a generic ester (*p*NPA) but does not exhibit appreciable biochemical activity toward either enantiomer of GR24, and this lack of biochemical activity toward GR24 is reflected in whole-plant responses. This information shows that like At-KAI2, Sm-KAI2a is unlikely to be a receptor for canonical SLs derived from carlactone. Nevertheless, complementation of *kai2* seedlings and rosettes by Sm-KAI2a implies that there exists an endogenous ligand common to both *S. moellendorffii* and Arabidopsis that is not a canonical SL but whose perception does depend on a receptor with an active site serine. Sm-KAI2a seems to have a much more restrictive specificity for its ligand than does At-KAI2, which can mediate responses to exogenous karrikins, debranones, and non-natural stereoisomers of SLs. The significance of this distinction is not clear, but potentially the wider ligand range for At-KAI2 might represent a gain of function within the angiosperms. Increased flexibility for ligand recognition might provide greater signaling flexibility, either for endogenous compounds or for exogenous compounds derived from, for example, smoke or commensal soil organisms.

### What Is the Function of KAI2 in Basal Land Plants?

Neither *M. polymorpha* KAI2 homolog could complement Arabidopsis *kai2*, which could either result from a shift in ligand preferences between Mp-KAI2s and At-KAI2 or from incompatibility of Mp-KAI2s with Arabidopsis signaling components. However, *M. polymorpha* gametophytes exhibit morphological responses to *rac*-GR24 (Delaux et al., 2012). We now know that Mp-KAI2b is active toward GR24$^{ent\text{-}5DS}$, as is At-KAI2 (Figure 4C), making it likely that a KAI2-dependent butenolide signaling system exists in *M. polymorpha*. Therefore, the inability of *M. polymorpha* KAI2 proteins to function in an Arabidopsis context most probably reflects substantial evolutionary changes among signaling components, such as the SMXL family.

Several SLs have been detected from *M. polymorpha* (Delaux et al., 2012) and *P. patens* (Proust et al., 2011). How do these SLs operate in basal land plants that lack D14 and D53-like proteins? It is reasonable to assume that these SLs have a developmental function because the SL-deficient *P. patens ccd8* mutant exhibits a number of growth anomalies (Proust et al., 2011; Delaux et al., 2012). Presumably KAI2 homologs act as receptor proteins for SLs in these species. SLs may act independently of a MAX2 homolog because KAI2 homologs are present in algae, but MAX2 arose within the land plant lineage and is apparently not involved in the SL response in *P. patens* (de Saint Germain et al., 2013). Therefore, it seems plausible that there is an evolutionarily ancient SL signaling pathway that does not depend on the angiosperm D14-MAX2-D53 core system (Bennett and Leyser, 2014). Accordingly, we speculate that there exist two broad kinds of butenolide signaling pathways in land plants. Both use a KAI2 homolog as a receptor protein. One is based on canonical, carlactone-derived SLs. In plants, such as mosses and liverworts, this pathway may not operate through

MAX2 and is involved in regulating cell growth and division to modulate filament elongation. At some point during the evolution of vascular plants, a KAI2 homolog became specialized to perceive and hydrolyze canonical SLs and to interact with MAX2 and an expanding family of SMXL proteins. This KAI2 homolog likely gave rise to the D14 clade and took on aspects of development influenced by SLs in angiosperms, such as shoot branching. In *S. moellendorffii*, Sm-KAI2b may belong to this pathway, based on its biochemical activity and phylogenetic position. Consistent with this notion, Challis et al. (2013) demonstrated that a *S. moellendorffii* MAX1 ortholog could functionally complement the strigolactone-deficient *max1* mutant of Arabidopsis, providing good evidence for the existence of a canonical biosynthetic pathway for strigolactones in *S. moellendorffii*. The other pathway, assumed to be ancestral, is based upon a different, non-SL ligand that is conserved across all land plants and uses Sm-KAI2a in *S. moellendorffii* and KAI2 in Arabidopsis. This ancestral system is presumably active in mosses and liverworts, and this system may also operate independently of MAX2 in these plants; tantalizingly, the degradation of KAI2 in Arabidopsis might indicate one element of this ancestral signaling system that still remains independent of MAX2 (Waters et al., 2015). Recently, it was shown that *P. patens* does not show any morphological response to $KAR_1$ despite having multiple putative KAI2 homologs (Hoffmann et al., 2014), suggesting that, if Sm-KAI2a is at all indicative, the ancestral pathway in basal land plants has more constrained ligand requirements. Coupled with a thorough evolutionary analysis of the SMXL family, firmer conclusions regarding the mechanisms and function of KAI2 homologs in basal land plants would be helped enormously by knockout mutagenesis, for which *M. polymorpha* represents a tractable system (Sugano et al., 2014).

## METHODS

### Plant Material and Growth Conditions

*Arabidopsis thaliana* was grown in 8-cm pots containing a 6:1:1 mixture of peat-based compost (Seedling Substrate Plus; Bord Na Mona), vermiculite, and perlite, respectively. Light was provided by white fluorescent lamps emitting 120 to 150 µmol photons $m^{-2}$ $s^{-1}$ with a 16-h-light/8-h-dark photoperiod, together with a 22°C light/16°C dark temperature cycle and constant 60% relative humidity.

The *kai2-1*, *kai2-2* (both L*er* background), and *d14-1* (Col-0 background) mutants were described previously (Waters et al., 2012a). The *d14-1 kai2-2* double mutant was introgressed into the L*er* background as follows. The *d14 kai2* double mutant (Col-0/L*er* hybrid) was backcrossed to L*er*, and *d14-1/D14* heterozygotes among the F1 were identified by PCR as described (Waters et al., 2012a). A single heterozygote was crossed again to L*er*, an F1 heterozygote selected, and the process repeated twice more. Finally, an *d14-1/D14* heterozygote from the fourth backcross was crossed once more with *kai2-2*, yielding a total of six crosses of the *d14-1* allele into the L*er* background. The resulting F1 was selfed. Homozygous wild-type, *d14-1*, *kai2-2*, and *d14 kai2* siblings were isolated from the segregating F2 progeny, and F3 plants were used for crossing and experiments. To introduce the *KAI2pro:*Sm-*KAI2a* transgene into the *d14 kai2* (L*er*) background from its original *kai2-2* (L*er*) background, two independent *KAI2pro:*Sm-*KAI2a* homozygous lines were each crossed with the introgressed *d14 kai2* (L*er*) double mutant. F2 seed was sown on 0.5× Murashige and Skoog (MS) medium supplemented with 20 $\mu g \cdot mL^{-1}$ hygromycin B to select for the *KAI2pro:*Sm-*KAI2a* transgene, resistant seedlings were transferred to soil, and *d14-1* homozygotes were selected based on the shoot branching phenotype. Finally, *KAI2pro:*Sm-*KAI2a* (*d14 kai2*) homozygotes were identified in the F4 generation by selection on hygromycin B, and this generation was used for experiments.

### Chemical Synthesis and Purification of Stereoisomers

Karrikins $KAR_1$ and $KAR_2$ were synthesized as described previously (Goddard-Borger et al., 2007). *rac*-GR24 was synthesized and separated into the two enantiomers $GR24^{5DS}$ and $GR24^{ent\text{-}5DS}$ by chiral HPLC as previously described (Scaffidi et al., 2014).

### Molecular Cloning

Oligonucleotide sequences are listed in Supplemental Table 1.

#### *Promoter Swaps*

The Arabidopsis *D14* promoter sequence, comprising 125 bp of the 3′ untranslated region (UTR) from the previous gene (At3g03980), 20 bp of the *D14* 5′ UTR, and 560 bp of the intervening sequence, was amplified using oligonucleotides MW361 and MW362. Amplification was performed using Phusion polymerase and genomic DNA from L*er* as a template. The purified PCR product was cloned into pCR2.1-TOPO (Life Technologies) and verified by sequencing. The *AtD14* promoter sequence was excised with *Hind*III and *Asc*I, and cloned into pMDC43 (Curtis and Grossniklaus, 2003) from which the CaMV *35S* promoter and *mGFP6* coding sequences were removed by digestion with *Hind*III and *Asc*I. This procedure yielded a Gateway-compatible binary Destination vector (pD14pro-GW). The Arabidopsis *KAI2* promoter sequence, comprising 110 bp of the 5′ UTR and 776 bp before the start codon of the adjacent gene (At4g37480), was amplified using oligonucleotides MW363 and MW364 and cloned using identical procedures, yielding the Destination vector pKAI2pro-GW (Waters et al., 2015).

The full-length *D14* coding sequence was amplified initially using oligonucleotides MW331 and MW332, and then with MW335 and MW336 to add Gateway attB sites, before cloning into pDONR207 (Life Technologies). The full-length *KAI2* coding sequence was cloned into pDONR207 as described previously (Waters and Smith, 2013). The two pDONR207 clones were recombined with pD14pro-GW and pKAI2pro-GW to generate the four promoter-coding sequence combinations.

#### *KAI2 and D14 Mutagenesis*

Site-directed mutagenesis of Ser-95 in KAI2 was performed as described previously (Waters et al., 2015). Mutagenesis of Ser-97 in D14 was performed by generating two PCR products that overlapped at the mutated site (using oligonucleotides MW483 and MW482, and MW481 and MW484, respectively). These products were purified, diluted 1:100, mixed, and used in a second round of PCR with MW481 and MW482. This product was cloned directly into pE-SUMO Amp (LifeSensors) and confirmed by DNA sequencing.

#### *Cloning of Selaginella moellendorffii and Marchantia polymorpha KAI2 Homologs*

Sm-KAI2a, Sm-KAI2b, Mp-KAI2a, and Mp-KAI2b proteins were identified by homology searches as described previously (Waters et al., 2012a). DNA sequences encoding Sm-KAI2a (GenBank Protein ID: 302782089) and Sm-KAI2b (302771439) were identified from the *S. moellendorffii* genome data sets (Banks et al., 2011; Waters et al., 2012a). The predicted

coding sequences, complete with flanking Gateway attB1 and attB2 sites, were codon-optimized for expression in Arabidopsis and synthesized by GenScript. The two sequences were recombined with pD14pro-GW and pKAI2pro-GW to generate the four promoter-coding sequence combinations.

DNA constructs encoding GFP fusions with Sm-KAI2a and Sm-KAI2a S95A (Figure 9) were constructed using Gibson assembly (Gibson et al., 2009). Briefly, the binary vector backbone was prepared by digesting pKAI2pro-Sm-KAI2a with *Asc*I and *Sac*I, which excised the Sm-KAI2a coding sequence while leaving the *KAI2* promoter and *nos* terminator intact. Overlapping PCR products encoding mGFP6 (oligonucleotides MW631 and MW632) and Sm-KAI2a (oligonucleotides MW633 and MW634) were then assembled directly into the purified vector fragment. The mutagenized Sm-KAI2a S94A coding sequence was generated as two PCR fragments (oligonucleotides MW633 and MW630, and oligonucleotides MW629 and MW634) that overlapped around Ser-94. These were mixed with the mGFP6 and vector fragments, and all assembled in a single step. In both assemblies, the DNA fragments overlapped by 23 to 28 bp and were generated using Phusion polymerase. The mGFP6 and Sm-KAI2a coding sequences were linked via a Gly-Ser-Gly tripeptide. Both constructs were verified by DNA sequencing.

Mp-KAI2a and Mp-KAI2b were identified from unpublished genome sequence data courtesy of John Bowman (Monash University, VIC, Australia). Predicted coding sequences were obtained by RT-PCR using DNase-treated RNA extracted from *M. polymorpha* gametophytes. Mp-*KAI2a* was amplified using Phusion DNA polymerase with oligonucleotides MW357 and MW358, and Mp-*KAI2b* with MW359 and MW360. A second round of PCR with MW335 and MW336 generated attB-flanked PCR products that were cloned into pDONR207. After sequence verification, the two coding sequences were recombined with pD14pro-GW and pKAI2pro-GW to generate the four promoter-coding sequence combinations.

### Plant Transformation

Homozygous *kai2-2* and *d14-1* plants were transformed by floral dip. Primary transgenic seedlings were selected on sterile 0.5× MS medium supplemented with 20 $\mu g \cdot mL^{-1}$ hygromycin B. T2 lines exhibiting a 3:1 ratio of hygromycin resistant-to-sensitive seedlings were propagated further to identify homozygous lines in the T3 generation. Experiments were performed using T3 and T4 generations.

### RNA Extraction and Transcript Analysis

Total RNA was extracted from Arabidopsis seedlings and *M. polymorpha* gametophytes using the RNeasy procedure (Qiagen). To prepare RNA from Arabidopsis seed, 40 mg of dry seed was imbibed in 1 mL of sterile water for 24 h at 20°C in constant white light with gentle end-over-end rotation. The seed were pelleted by centrifugation for 5 min at 6000*g* and the water removed by pipetting. The seed were snap-frozen in liquid nitrogen and ground to a fine powder using a pestle and mortar. RNA was extracted using the Spectrum Plant Total RNA Kit (Sigma-Aldrich) using Protocol A as specified by the manufacturer.

RNA was treated with TURBO DNase (Life Technologies). For quantitative PCR, 500 ng total RNA was reverse transcribed using the iScript cDNA Synthesis Kit (Bio-Rad) and then diluted 3-fold with nuclease-free water. For cloning purposes, RNA was converted to cDNA using SuperScript III reverse transcriptase and oligo(dT) primer (Life Technologies).

Quantitative PCR was performed as described previously (Waters and Smith, 2013). The choice of reference transcripts was based on those identified by Czechowski et al. (2005). Primers were designed using QuantPrime software (Arvidsson et al., 2008) or, in the case of *M. polymorpha* and *S. moellendorffii* genes, using Primer3 software (Untergasser et al., 2012). Oligonucleotide sequences are listed in Supplemental Table 1.

### Hypocotyl Elongation Assays

Hypocotyl elongation assays were performed under red light as described previously (Waters et al., 2012a).

### Seed Germination Assays

Seeds were harvested in triplicate batches from parents grown under identical conditions in randomized positions within a tray. Each batch comprised the seeds from three to four parents. Plants were watered until flowering ceased, and seeds were collected when the last siliques started to turn yellow. Seeds were dried under silica gel (22°C, relative humidity 15 to 20%) for 3 to 4 d and then stored at –80°C until use. For germination assays, seeds were surface-sterilized with 70% ethanol + 0.05% Tween 20 for 5 min, rinsed once with 100% ethanol, and allowed to dry. The seeds were sprinkled on sterile 1% Phytagel (Sigma-Aldrich) in aqueous 2 mM $MgCl_2$. Plates were incubated under constant light (100 $\mu mol\ m^{-2}\ s^{-1}$ from fluorescent white tubes) at 21°C for 5 d, and germination (radicle emergence) was scored daily.

### Analysis of Leaf Morphology

Plants were grown under long-day conditions as described above, and leaves 4, 5, and 6 were harvested for image analysis 24 d postgermination (dpg). Leaf image acquisition, processing, and analysis using LeafAnalyser (Weight et al., 2008) and ImageJ (http://rsb.info.nih.gov/ij) were described previously (Scaffidi et al., 2013). Leaf length was defined by the distance between the leaf apex and base of the petiole. The leaf midpoint was defined manually by drawing a line, perpendicular to the proximal-distal axis, across the lamina at its widest point. Straight-line distances were then measured from this line to the leaf apex.

### In Vitro Hydrolysis Assays

Hydrolysis assays with *p*NPA were performed in 20 mM HEPES, pH 7.5, 150 mM NaCl, and 10% glycerol, using 0.0125 mg/mL protein. *p*NPA was dissolved in DMSO and diluted in the assay buffer such that the final concentration of DMSO was held constant at 1%. Reactions were incubated at 30°C and monitored for generation of *p*-nitrophenol by absorbance at 405 nm. Natural hydrolysis by buffer alone was determined to follow the linear equation $v_{i\,(buffer)} = 0.0115^*[S]$ ($R^2 = 0.9996$), where $v_i$ is the initial speed of hydrolysis (abs. units/min) and [*S*] is the concentration of substrate (mM). The effects of the buffer and enzyme were assumed to be additive such that $v_{i\,(enzyme)} = v_{i\,(observed)} - v_{i\,(buffer)}$. Michaelis-Menten kinetic parameters were approximated from Hanes-Woolf plots.

$GR24^{5DS}$ and $GR24^{ent\text{-}5DS}$ in DMSO (2.5 µL, 10 mM) were each added to separate solutions of each protein (50 µL, 2 $mg \cdot mL^{-1}$ in 20 mM HEPES, 150 mM NaCl, and 10% glycerol, pH 7.5). The reactions were monitored at 22°C using a Hewlett-Packard 1050 HPLC system fitted with a multi-wavelength detector and a C18 reversed-phase column (Grace-Davison, Alltima C18; particle size of 5 µm, internal diameter of 2.1 mm, and length of 150 mm). Samples were analyzed at 0 and 2 h by injecting 10 µL and eluting under gradient conditions commencing at 10% acetonitrile:water and increasing to 80% acetonitrile:water at 10 min; holding for 2 min and reequilibrating for 3 min using a flow rate of 0.3 $mL \cdot min^{-1}$. The consumption of $GR24^{5DS}$ and $GR24^{ent\text{-}5DS}$ was monitored at 240 nm.

### Differential Scanning Fluorimetry

Proteins (40 µM) and SYPRO Tangerine protein reporter dye (10×, diluted from 500× stock in DMSO as purchased) were diluted into buffer (20 mM HEPES, pH 7.5, and 150 mM NaCl). Ligand was diluted 1:10 into the same buffer from 20× stocks in acetone. Five microliters of protein and dye solution were combined with 5 µL of ligand solution in a 384-well, white

microtiter plate such that final reactions contained 20 μM protein, 5× dye, 0 to 200 μM ligand, and 5% (v/v) acetone. Plates were incubated in darkness for 30 min before analysis on a Roche LC480 thermocycler using the following settings: excitation 483 nm, emission 640 nm, and ramp from 20 to 80°C with 20 acquisitions per minute (corresponding to a rate of temperature increase of ~0.2°C/s). Data were processed using the "Tm calling" function within the LC480 software, which plots temperature against the first derivative of fluorescence over temperature. The curve data for each sample was imported into Microsoft Excel, where averages of the technical replicates were calculated and the graphs generated. Each protein-ligand combination was replicated four times on the same plate, and each experiment was performed at least twice.

### Protein Expression and Purification

Full-length coding sequences, identical to those used in plant expression vectors, were ligated into the *Bam*HI and *Xho*I sites of pE-SUMO Amp. Procedures for expression and purification were identical for all fusion proteins. Positive clones were sequenced and transformed into Rosetta DE3 pLysS cells (Novagen). Two to three colonies were inoculated into 5 mL Luria-Bertani medium containing 100 μg/mL carbenicillin and 34 μg/mL chloramphenicol, and grown for 14 to 16 h at 30°C with shaking (180 rpm). Duplicate 2-liter flasks containing 450 mL Luria-Bertani medium and 50 μg/mL carbenicillin were inoculated with 450 μL of the overnight culture, and incubated at 30°C/180 rpm for ~6 h until the optical density at 600 nm reached 0.8 to 1.0. The cultures were chilled at 4°C for 10 to 15 min, expression induced with 0.1 mM isopropyl β-D-1-thiogalactopyranoside, and growth continued overnight (16 h) at 16°C/180 rpm. Cultures were harvested by centrifugation and stored at –80°C.

Bacterial pellets from a total of 900 mL of culture were resuspended in 25 mL of lysis buffer comprising 20 mM HEPES, pH 7.5, 150 mM NaCl, 10% (v/v) glycerol, 20 mM imidazole, 1× BugBuster reagent (Novagen), and 25 units of Benzonase nuclease (Novagen). Lysates were clarified by two successive centrifugations at 16,000*g* for 30 min each. The clarified lysates were loaded onto a 30-mL Econo-Pac gravity chromatography column (Bio-Rad) containing 2 mL (settled volume) of Ni-NTA resin (Novagen), preequilibrated with wash buffer (20 mM HEPES, pH 7.5, 150 mM NaCl, 10% [v/v] glycerol, and 20 mM imidazole). Lysates were incubated on the column with end-over-end rotation (15 rpm) at 4°C for 60 min, and then the column was drained. The resin was washed twice with 25 mL of ice-cold wash buffer. Bound proteins were eluted in successive 1-mL fractions with ice-cold 20 mM HEPES, pH 7.5, 150 mM NaCl, 10% (v/v) glycerol, and 200 mM imidazole. Fractions containing recombinant protein were combined and concentrated to <1 mL with an Amicon Ultra-4 centrifugal device (Millipore) with 10-kD molecular weight cutoff. To remove imidazole, the concentrated protein was buffer-exchanged into 20 mM HEPES, pH 7.5, 150 mM NaCl, and 10% (v/v) glycerol using a 2-mL Zeba Spin desalting column (Thermo Scientific). Finally, protein concentration was estimated using Quick Start Bradford 1× dye reagent (Bio-Rad) and BSA standards. Protein purity was assessed by SDS-PAGE (Supplemental Figure 5).

### Protein Extraction and Immunoblotting

Approximately 100 mg of whole 7-d-old Arabidopsis seedlings, or 50 mg of dry seeds imbibed in water for 24 h, were snap-frozen in liquid nitrogen and ground using a mortar and pestle. Soluble proteins from seedlings were extracted using 150 μL of lysis buffer (50 mM Tris, pH 7.5, 150 mM NaCl, 10% glycerol, 0.1% Tween 20, 1 mM PMSF, 1 mM DTT, and 1× Complete protease inhibitors [Roche]). Lysates were clarified by two successive centrifugations at 20,000*g* for 5 min each. For seed, 300 μL of lysis buffer was added to frozen powder, vortexed thoroughly, and centrifuged as above to pellet debris and separate the aqueous phase from the oil phase, which was discarded. Protein concentration was estimated as described above. Proteins were separated by 12% SDS-PAGE and blotted onto Hybond-P membrane (GE Healthcare). Immunoblotting procedures and generation of the anti-At-KAI2 antibody were described previously (Waters et al., 2015). Chemiluminescence images (16-bit) were collected with an ImageQuantRT ECL system (GE Healthcare). Band intensity was calculated using the gel analysis functions of ImageJ by calculating the area under each peak and adjusting for loading with reference to α-tubulin.

### Treatment of Seedlings in Liquid Culture

For Figure 7E, seedlings were grown on solidified 0.5× MS medium in ventilated, sterile plastic tubs for 14 d under long-day conditions as described above. On day 15, ~50 seedlings were transferred to a 250-mL Erlenmeyer flask containing 25 mL of liquid 0.5× MS medium. The flasks were returned to the same growth room and were shaken at 60 rpm overnight. On day 16, 5 μM $KAR_2$ or an equivalent volume of acetone was added and the seedlings harvested 24 h later. Each RNA sample corresponded to independent flasks of seedlings grown and treated in parallel. Seedlings were harvested by decanting, blotted dry, weighed, and snap-frozen in liquid nitrogen.

### Statistical Analysis

Significance groupings were determined using one-way ANOVAs based on Bonferroni (Dunn) *t* tests. For germination assays, data were arcsine-transformed prior to ANOVA. Analyses were performed using SAS Enterprise Guide v4.3.

### Accession Numbers

Sequence data from this article can be found in the Arabidopsis Genome Initiative or GenBank/EMBL databases under the following accession numbers: At-*D14* (At3g03990), *KAI2* (At4g37470), *DLK2* (At3g24420), *STH7* (At4g39070), *KUF1* (At1g31350), *IAA5* (At1g15580), *IAA6* (At1g52830), *CACS* (At5g46630), *TIP41L* (At4g34270), Sm-*KAI2a* (SELMODRAFT_441991), Sm-*KAI2b* (SELMODRAFT_267235), Mp-*KAI2a* (KJ409549), and Mp-*KAI2b* (KJ409550).

### Supplemental Data

**Supplemental Figure 1.** Overexpression of KAI2 enhances seed germination rates.

**Supplemental Figure 2.** Structural representation of key residues of Arabidopsis KAI2.

**Supplemental Figure 3.** Protein alignment of KAI2 and D14 homologs.

**Supplemental Figure 4.** Whole-gel blot demonstrating α-KAI2 specificity.

**Supplemental Figure 5.** SDS-PAGE of SUMO-KAI2 fusion proteins.

**Supplemental Figure 6.** Estimation of kinetic constants for activity of purified KAI2 homologs toward *p*NPA.

**Supplemental Figure 7.** Arabidopsis D14 hydrolyzes both enantiomers of *rac*-GR24.

**Supplemental Figure 8.** Karrikins do not induce a change in Arabidopsis KAI2 melting temperature.

**Supplemental Figure 9.** KAI2 homologs from *Marchantia polymorpha* are nonfunctional in Arabidopsis.

**Supplemental Table 1.** Oligonucleotides used in this study.

## ACKNOWLEDGMENTS

We thank Rowena Long and Santana Royan (University of Western Australia) for technical assistance and helpful discussion throughout the course of the work, David Nelson (University of Georgia) for comments and discussion, Tom Dierschke and John Bowman (Monash University, Melbourne) for supply of *M. polymorpha* spores and sequence data, and Rohan Bythell-Douglas and Charlie Bond (University of Western Australia) for advice on protein purification. This work was supported by the Australian Research Council (DP130103646).

## AUTHOR CONTRIBUTIONS

M.T.W., A.S., S.L.Y.M., Y.K.S., G.R.F., and S.M.S. designed the research. M.T.W., A.S., S.L.Y.M., and Y.K.S. performed research. A.S. and G.R.F. contributed new analytical tools. M.T.W., S.L.Y.M., and S.M.S. analyzed data. M.T.W. and S.M.S. wrote the article.

Received February 16, 2015; revised June 18, 2015; accepted June 29, 2015; published July 14, 2015.

## REFERENCES

**Abe, S., et al.** (2014). Carlactone is converted to carlactonoic acid by MAX1 in Arabidopsis and its methyl ester can directly interact with AtD14 in vitro. Proc. Natl. Acad. Sci. USA **111:** 18084–18089.

**Arite, T., Umehara, M., Ishikawa, S., Hanada, A., Maekawa, M., Yamaguchi, S., and Kyozuka, J.** (2009). d14, a strigolactone-insensitive mutant of rice, shows an accelerated outgrowth of tillers. Plant Cell Physiol. **50:** 1416–1424.

**Arvidsson, S., Kwasniewski, M., Riaño-Pachón, D.M., and Mueller-Roeber, B.** (2008). QuantPrime–a flexible tool for reliable high-throughput primer design for quantitative PCR. BMC Bioinformatics **9:** 465.

**Banks, J.A., et al.** (2011). The Selaginella genome identifies genetic changes associated with the evolution of vascular plants. Science **332:** 960–963.

**Bennett, T., and Leyser, O.** (2014). Strigolactone signalling: standing on the shoulders of DWARFs. Curr. Opin. Plant Biol. **22:** 7–13.

**Bowman, J.L.** (2013). Walkabout on the long branches of plant evolution. Curr. Opin. Plant Biol. **16:** 70–77.

**Bythell-Douglas, R., Waters, M.T., Scaffidi, A., Flematti, G.R., Smith, S.M., and Bond, C.S.** (2013). The structure of the karrikin-insensitive protein (KAI2) in *Arabidopsis thaliana*. PLoS One **8:** e54758.

**Challis, R.J., Hepworth, J., Mouchel, C., Waites, R., and Leyser, O.** (2013). A role for more axillary growth1 (MAX1) in evolutionary diversity in strigolactone signaling upstream of MAX2. Plant Physiol. **161:** 1885–1902.

**Chevalier, F., Nieminen, K., Sánchez-Ferrero, J.C., Rodríguez, M.L., Chagoyen, M., Hardtke, C.S., and Cubas, P.** (2014). Strigolactone promotes degradation of DWARF14, an $\alpha/\beta$ hydrolase essential for strigolactone signaling in Arabidopsis. Plant Cell **26:** 1134–1150.

**Cook, C.E., Whichard, L.P., Turner, B., Wall, M.E., and Egley, G.H.** (1966). Germination of witchweed (*Striga lutea* Lour.): Isolation and properties of a potent stimulant. Science **154:** 1189–1190.

**Curtis, M.D., and Grossniklaus, U.** (2003). A Gateway cloning vector set for high-throughput functional analysis of genes in planta. Plant Physiol. **133:** 462–469.

**Czechowski, T., Stitt, M., Altmann, T., Udvardi, M.K., and Scheible, W.-R.** (2005). Genome-wide identification and testing of superior reference genes for transcript normalization in Arabidopsis. Plant Physiol. **139:** 5–17.

**Delaux, P.-M., Xie, X., Timme, R.E., Puech-Pages, V., Dunand, C., Lecompte, E., Delwiche, C.F., Yoneyama, K., Bécard, G., and Séjalon-Delmas, N.** (2012). Origin of strigolactones in the green lineage. New Phytol. **195:** 857–871.

**de Saint Germain, A., Bonhomme, S., Boyer, F.-D., and Rameau, C.** (2013). Novel insights into strigolactone distribution and signalling. Curr. Opin. Plant Biol. **16:** 583–589.

**Deshaies, R.J., and Joazeiro, C.A.P.** (2009). RING domain E3 ubiquitin ligases. Annu. Rev. Biochem. **78:** 399–434.

**Flematti, G.R., Ghisalberti, E.L., Dixon, K.W., and Trengove, R.D.** (2004). A compound from smoke that promotes seed germination. Science **305:** 977.

**Flematti, G.R., Ghisalberti, E.L., Dixon, K.W., and Trengove, R.D.** (2009). Identification of alkyl substituted 2H-furo[2,3-c]pyran-2-ones as germination stimulants present in smoke. J. Agric. Food Chem. **57:** 9475–9480.

**Fukui, K., Ito, S., Ueno, K., Yamaguchi, S., Kyozuka, J., and Asami, T.** (2011). New branching inhibitors and their potential as strigolactone mimics in rice. Bioorg. Med. Chem. Lett. **21:** 4905–4908.

**Gibson, D.G., Young, L., Chuang, R.-Y., Venter, J.C., Hutchison III, C.A., and Smith, H.O.** (2009). Enzymatic assembly of DNA molecules up to several hundred kilobases. Nat. Methods **6:** 343–345.

**Goddard-Borger, E.D., Ghisalberti, E.L., and Stick, R.V.** (2007). Synthesis of the germination stimulant 3-methyl-2H-furo[2,3-c]pyran-2-one and analogous compounds from carbohydrates. Eur. J. Org. Chem. **2007:** 3925–3934.

**Guo, Y., Zheng, Z., La Clair, J.J., Chory, J., and Noel, J.P.** (2013). Smoke-derived karrikin perception by the $\alpha/\beta$-hydrolase KAI2 from Arabidopsis. Proc. Natl. Acad. Sci. USA **110:** 8284–8289.

**Hamiaux, C., Drummond, R.S., Janssen, B.J., Ledger, S.E., Cooney, J.M., Newcomb, R.D., and Snowden, K.C.** (2012). DAD2 is an $\alpha/\beta$ hydrolase likely to be involved in the perception of the plant branching hormone, strigolactone. Curr. Biol. **22:** 2032–2036.

**Hoffmann, B., Proust, H., Belcram, K., Labrune, C., Boyer, F.-D., Rameau, C., and Bonhomme, S.** (2014). Strigolactones inhibit caulonema elongation and cell division in the moss *Physcomitrella patens*. PLoS One **9:** e99206.

**Ishikawa, S., Maekawa, M., Arite, T., Onishi, K., Takamure, I., and Kyozuka, J.** (2005). Suppression of tiller bud activity in tillering dwarf mutants of rice. Plant Cell Physiol. **46:** 79–86.

**Jiang, L., et al.** (2013). DWARF 53 acts as a repressor of strigolactone signalling in rice. Nature **504:** 401–405.

**Kagiyama, M., Hirano, Y., Mori, T., Kim, S.-Y., Kyozuka, J., Seto, Y., Yamaguchi, S., and Hakoshima, T.** (2013). Structures of D14 and D14L in the strigolactone and karrikin signaling pathways. Genes Cells **18:** 147–160.

**Kameoka, H., and Kyozuka, J.** (2015). Downregulation of rice *DWARF 14 LIKE* suppress mesocotyl elongation via a strigolactone independent pathway in the dark. J. Genet. Genomics **42:** 119–124.

**Nakamura, H., et al.** (2013). Molecular mechanism of strigolactone perception by DWARF14. Nat. Commun. **4:** 2613.

**Nelson, D.C., Flematti, G.R., Ghisalberti, E.L., Dixon, K.W., and Smith, S.M.** (2012). Regulation of seed germination and seedling growth by chemical signals from burning vegetation. Annu. Rev. Plant Biol. **63:** 107–130.

**Nelson, D.C., Flematti, G.R., Riseborough, J.-A., Ghisalberti, E.L., Dixon, K.W., and Smith, S.M.** (2010). Karrikins enhance light responses during germination and seedling development in *Arabidopsis thaliana*. Proc. Natl. Acad. Sci. USA **107:** 7095–7100.

**Nelson, D.C., Riseborough, J.-A., Flematti, G.R., Stevens, J., Ghisalberti, E.L., Dixon, K.W., and Smith, S.M.** (2009). Karrikins discovered in smoke trigger Arabidopsis seed germination by a mechanism requiring gibberellic acid synthesis and light. Plant Physiol. **149:** 863–873.

**Nelson, D.C., Scaffidi, A., Dun, E.A., Waters, M.T., Flematti, G.R., Dixon, K.W., Beveridge, C.A., Ghisalberti, E.L., and Smith, S.M.** (2011). F-box protein MAX2 has dual roles in karrikin and strigolactone signaling in *Arabidopsis thaliana*. Proc. Natl. Acad. Sci. USA **108:** 8897–8902.

**Niesen, F.H., Berglund, H., and Vedadi, M.** (2007). The use of differential scanning fluorimetry to detect ligand interactions that promote protein stability. Nat. Protoc. **2:** 2212–2221.

**Proust, H., Hoffmann, B., Xie, X., Yoneyama, K., Schaefer, D.G., Yoneyama, K., Nogué, F., and Rameau, C.** (2011). Strigolactones regulate protonema branching and act as a quorum sensing-like signal in the moss *Physcomitrella patens.* Development **138:** 1531–1539.

**Scaffidi, A., Waters, M.T., Bond, C.S., Dixon, K.W., Smith, S.M., Ghisalberti, E.L., and Flematti, G.R.** (2012). Exploring the molecular mechanism of karrikins and strigolactones. Bioorg. Med. Chem. Lett. **22:** 3743–3746.

**Scaffidi, A., Waters, M.T., Ghisalberti, E.L., Dixon, K.W., Flematti, G.R., and Smith, S.M.** (2013). Carlactone-independent seedling morphogenesis in Arabidopsis. Plant J. **76:** 1–9.

**Scaffidi, A., Waters, M.T., Sun, Y.K., Skelton, B.W., Dixon, K.W., Ghisalberti, E.L., Flematti, G.R., and Smith, S.M.** (2014). Strigolactone hormones and their stereoisomers signal through two related receptor proteins to induce different physiological responses in Arabidopsis. Plant Physiol. **165:** 1221–1232.

**Smith, S.M., and Li, J.** (2014). Signalling and responses to strigolactones and karrikins. Curr. Opin. Plant Biol. **21:** 23–29.

**Stanga, J.P., Smith, S.M., Briggs, W.R., and Nelson, D.C.** (2013). SUPPRESSOR OF MORE AXILLARY GROWTH2 1 controls seed germination and seedling development in Arabidopsis. Plant Physiol. **163:** 318–330.

**Stirnberg, P., Furner, I.J., and Ottoline Leyser, H.M.** (2007). MAX2 participates in an SCF complex which acts locally at the node to suppress shoot branching. Plant J. **50:** 80–94.

**Sugano, S.S., Shirakawa, M., Takagi, J., Matsuda, Y., Shimada, T., Hara-Nishimura, I., and Kohchi, T.** (2014). CRISPR/Cas9-mediated targeted mutagenesis in the liverwort *Marchantia polymorpha* L. Plant Cell Physiol. **55:** 475–481.

**Sun, X.-D., and Ni, M.** (2011). HYPOSENSITIVE TO LIGHT, an alpha/beta fold protein, acts downstream of ELONGATED HYPOCOTYL 5 to regulate seedling de-etiolation. Mol. Plant **4:** 116–126.

**Untergasser, A., Cutcutache, I., Koressaar, T., Ye, J., Faircloth, B.C., Remm, M., and Rozen, S.G.** (2012). Primer3–new capabilities and interfaces. Nucleic Acids Res. **40:** e115.

**Waldie, T., McCulloch, H., and Leyser, O.** (2014). Strigolactones and the control of plant development: lessons from shoot branching. Plant J. **79:** 607–622.

**Waters, M.T., and Smith, S.M.** (2013). KAI2- and MAX2-mediated responses to karrikins and strigolactones are largely independent of HY5 in Arabidopsis seedlings. Mol. Plant **6:** 63–75.

**Waters, M.T., Nelson, D.C., Scaffidi, A., Flematti, G.R., Sun, Y.K., Dixon, K.W., and Smith, S.M.** (2012a). Specialisation within the DWARF14 protein family confers distinct responses to karrikins and strigolactones in Arabidopsis. Development **139:** 1285–1295.

**Waters, M.T., Scaffidi, A., Flematti, G., and Smith, S.M.** (2015). Substrate-induced degradation of the α/β-fold hydrolase KARRIKIN INSENSITIVE 2 requires a functional catalytic triad but is independent of MAX2. Mol. Plant **8:** 814–817.

**Waters, M.T., Scaffidi, A., Flematti, G.R., and Smith, S.M.** (2012b). Karrikins force a rethink of strigolactone mode of action. Plant Signal. Behav. **7:** 969–972.

**Waters, M.T., Scaffidi, A., Flematti, G.R., and Smith, S.M.** (2013). The origins and mechanisms of karrikin signalling. Curr. Opin. Plant Biol. **16:** 667–673.

**Waters, M.T., Scaffidi, A., Sun, Y.K., Flematti, G.R., and Smith, S.M.** (2014). The karrikin response system of Arabidopsis. Plant J. **79:** 623–631.

**Weight, C., Parnham, D., and Waites, R.** (2008). LeafAnalyser: a computational method for rapid and large-scale analyses of leaf shape variation. Plant J. **53:** 578–586.

**Zhao, L.-H., et al.** (2013). Crystal structures of two phytohormone signal-transducing α/β hydrolases: karrikin-signaling KAI2 and strigolactone-signaling DWARF14. Cell Res. **23:** 436–439.

**Zhou, F., et al.** (2013). D14-SCF(D3)-dependent degradation of D53 regulates strigolactone signalling. Nature **504:** 406–410.